

Recent Standard Model Highlights

Savannah Clawson (DESY)

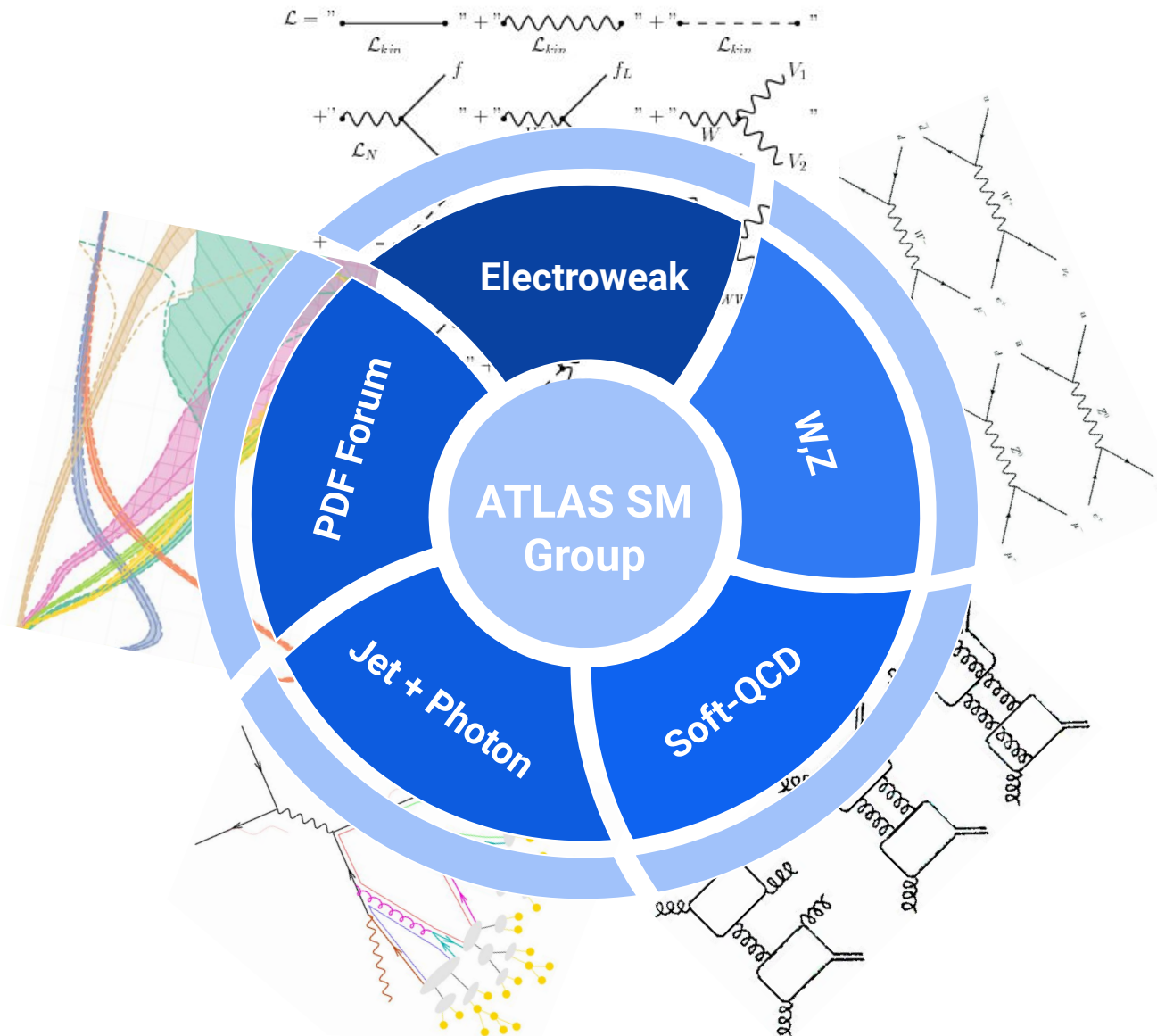
ATLAS-D 2024

Mainz

13th September 2024

HELMHOLTZ





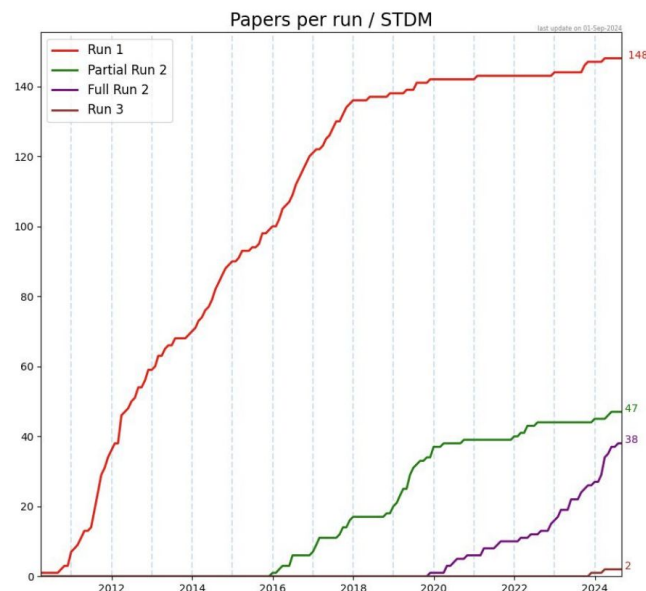
Introduction

Another productive year for the SM group

- **14 new results** since last ATLAS-D (excluding CONF conversions) covering a wide range of physics:
 - **Electroweak precision:** W boson mass and width, $Z \rightarrow l\bar{l}$ 8 TeV, W/Z run-3
 - **Hard QCD:** MET+jets, Z+HF, Z+jets multifold, R3/2
 - **Jet substructure:** Lund multiplicities, Track functions, Lund plane in ttbar
 - **Soft-QCD:** Strangeness of the underlying event
 - **Multiboson:** WZ polarisation high p_T , VBS $W\gamma$, VBS WZ
- + 9 CONF notes converted to paper

The first half of 2024 saw one of the highest paper submission rates in STDM history

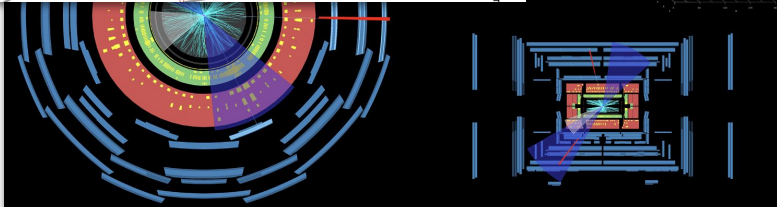
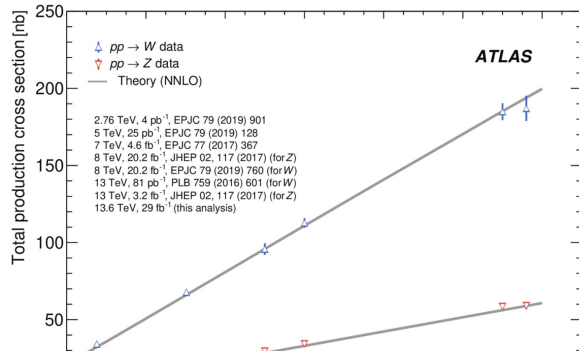
List of all published and ongoing SM analyses [here](#)



First ATLAS measurement of W and Z boson production using Run-3 data

28 March 2024 | By ATLAS Collaboration

For over 40 years, since their discovery at CERN's SPS collider, W^{\pm} and Z bosons have been the subject of extensive research. As the carriers of the weak force, precise measurements of their properties are essential for understanding the electroweak sector of the Standard Model and possibly also finding deviations from theory predictions, which would hint for new physics beyond the Standard Model. For instance, studying W and Z boson production in different energy regimes may unveil potential contributions from new particles or interactions, which are accessible at higher energies but invisible at low energies



[Updates](#) > [Briefing](#) > ATLAS explores Z boson production with heavy-flavour quarks

Physics Briefing

Tags:
Z boson,
physics results

ATLAS explores Z boson production with heavy-flavour quarks

15 April 2024 | By ATLAS Collaboration

Physics Briefing

Tags:
physics results,
lepton flavour universality,
Moriond 2024

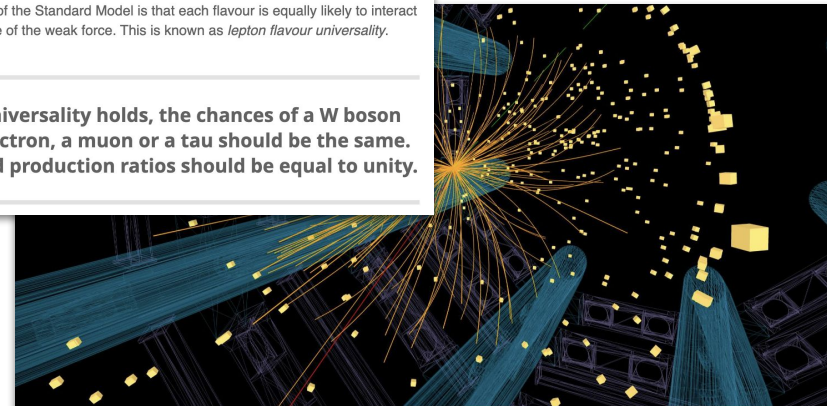
Measuring the delicate balance of lepton flavours

25 March 2024 | By ATLAS Collaboration

In a new result [presented](#) at the Moriond EW conference, physicists at the ATLAS Collaboration tested lepton flavour universality between muons and electrons. The precision of the result stands as the best yet-achieved in W-boson decays by a single experiment and surpasses the world average.

Most elementary particles can be categorised into groups or families with similar properties. For example, the lepton family includes the electron (e), which forms the negatively charged cloud of particles surrounding the nucleus in every atom; the muon (μ), a heavier particle found in cosmic rays; and the tau (τ), an even heavier short-lived particle only seen in high-energy particle interactions. As far as physicists know, the only difference between these particles is their mass. In particular, a remarkable feature of the Standard Model is that each flavour is equally likely to interact with a W boson, a carrier particle of the weak force. This is known as *lepton flavour universality*.

If lepton flavour universality holds, the chances of a W boson decaying into an electron, a muon or a tau should be the same. Thus, their measured production ratios should be equal to unity.



[Updates](#) > [Briefing](#) > ATLAS provides first measurement of the W-boson width at the LHC

Physics Briefing

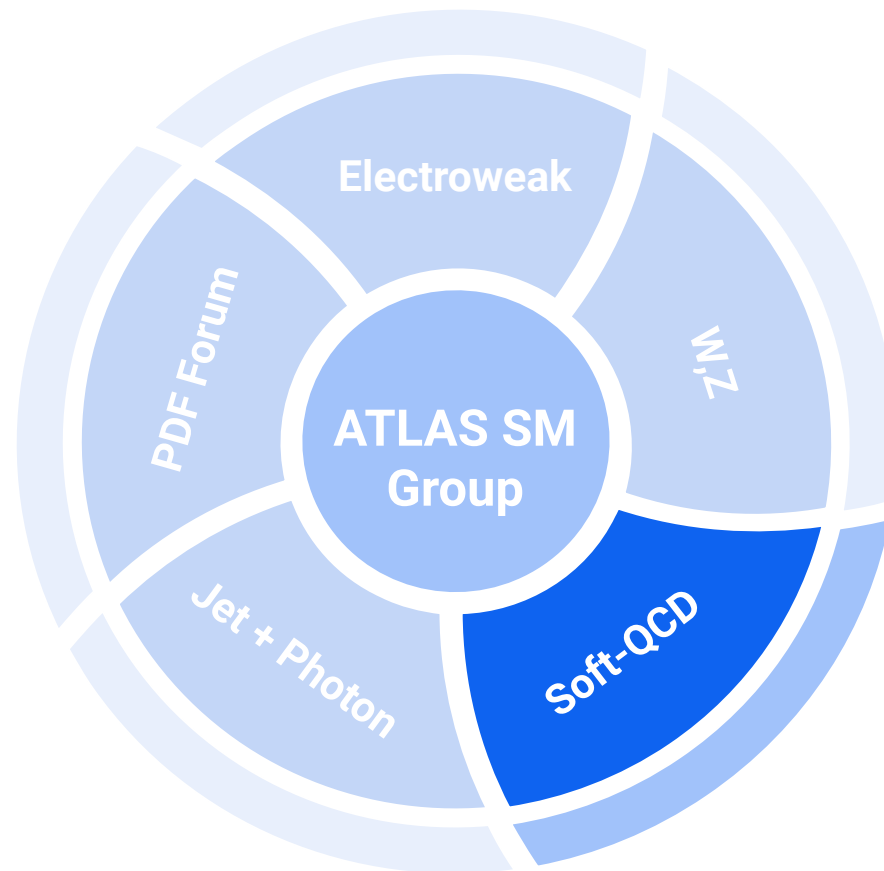
Tags:
W boson,
physics results

ATLAS provides first measurement of the W-boson width at the LHC

5 April 2024 | By ATLAS Collaboration

ATLAS SM subgroups

SMSoftQcdWorkingGroup

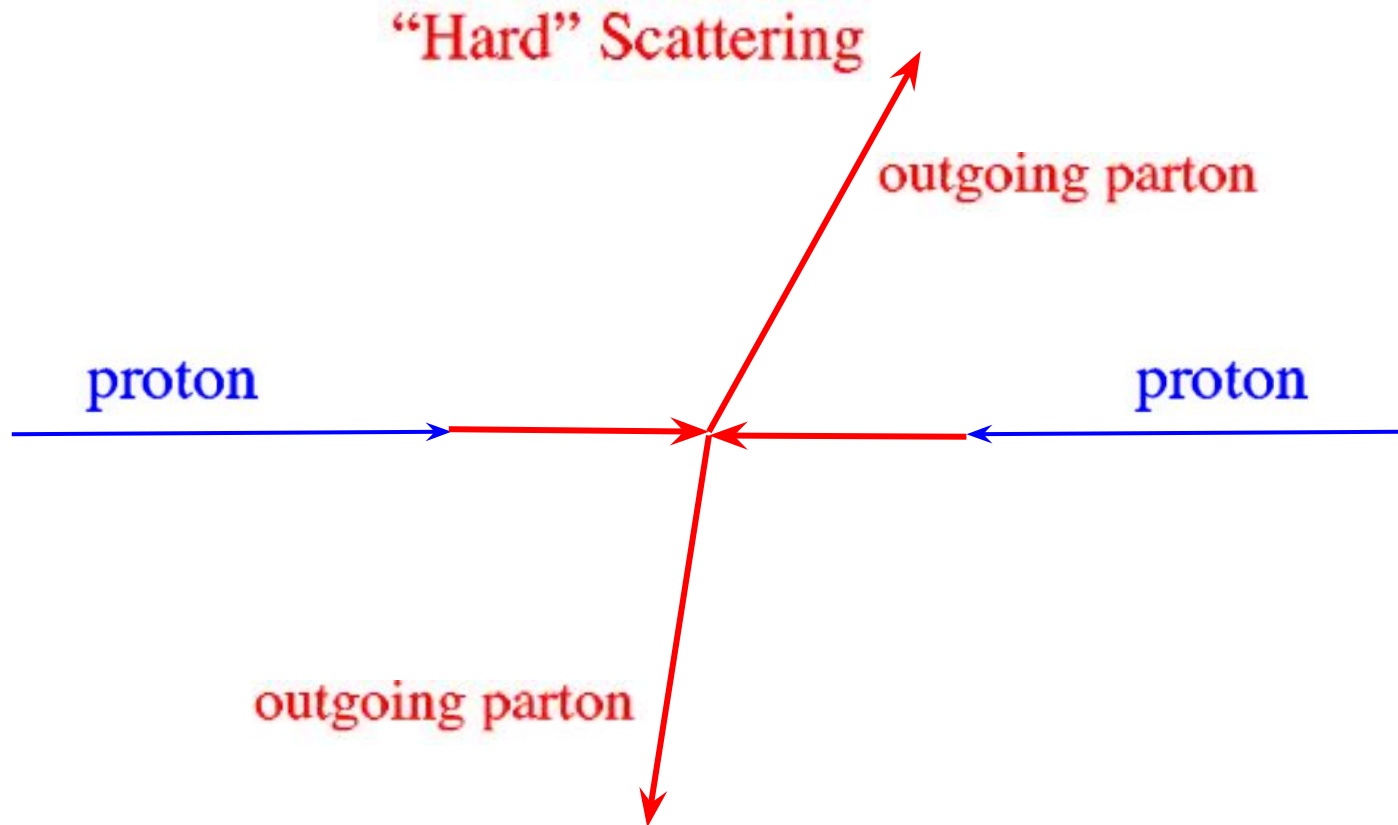


Group interests:

- Non-perturbative QCD
- Final state correlations
- Fragmentation and hadronisation
- Underlying event and event shape variables
- Diffractive processes
- Overlap with cosmic-ray physics
- Forward detectors

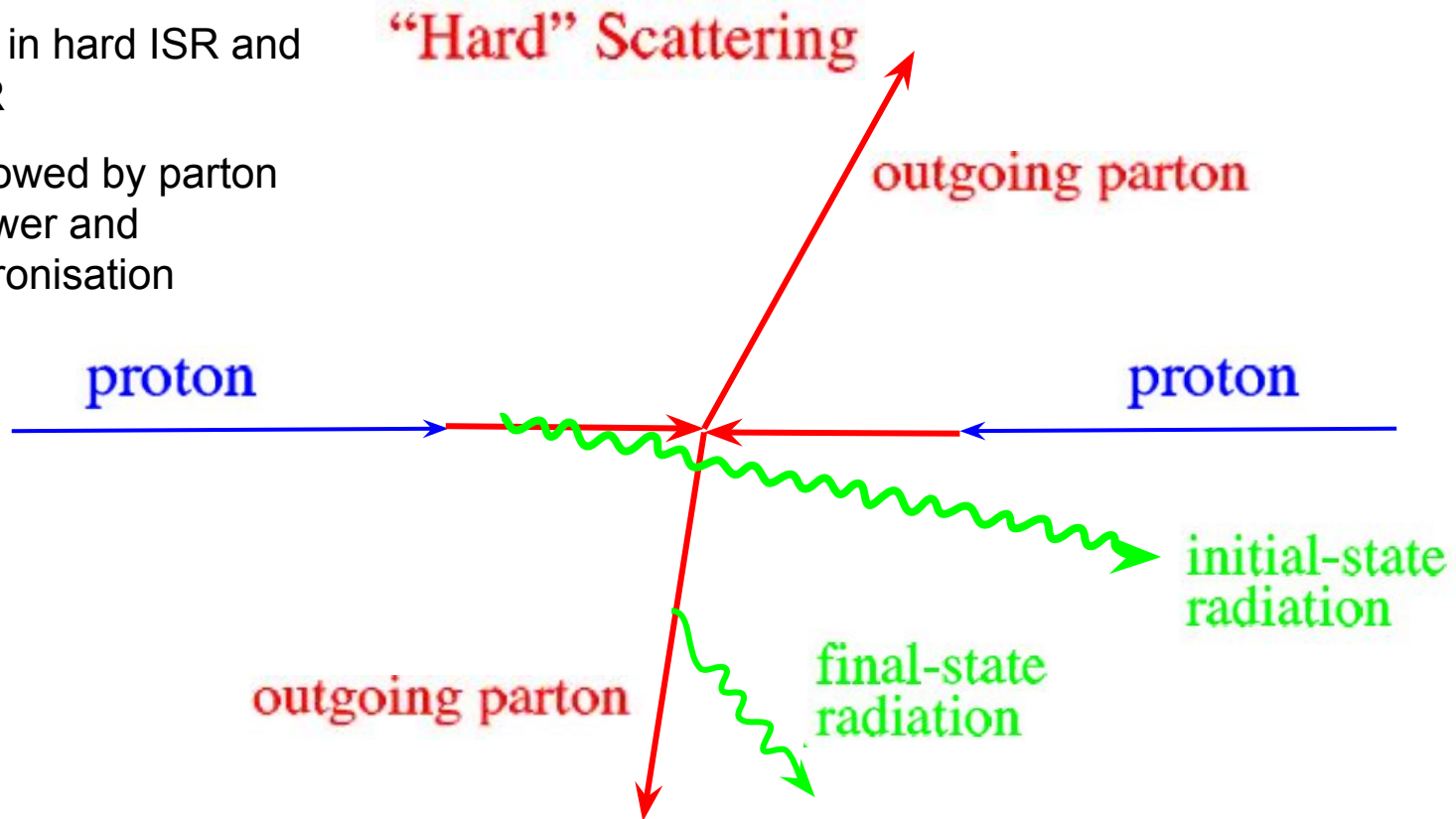
A “typical” LHC collision

- We’re usually interested in hard-scatter (HS) interactions between two partons within the protons



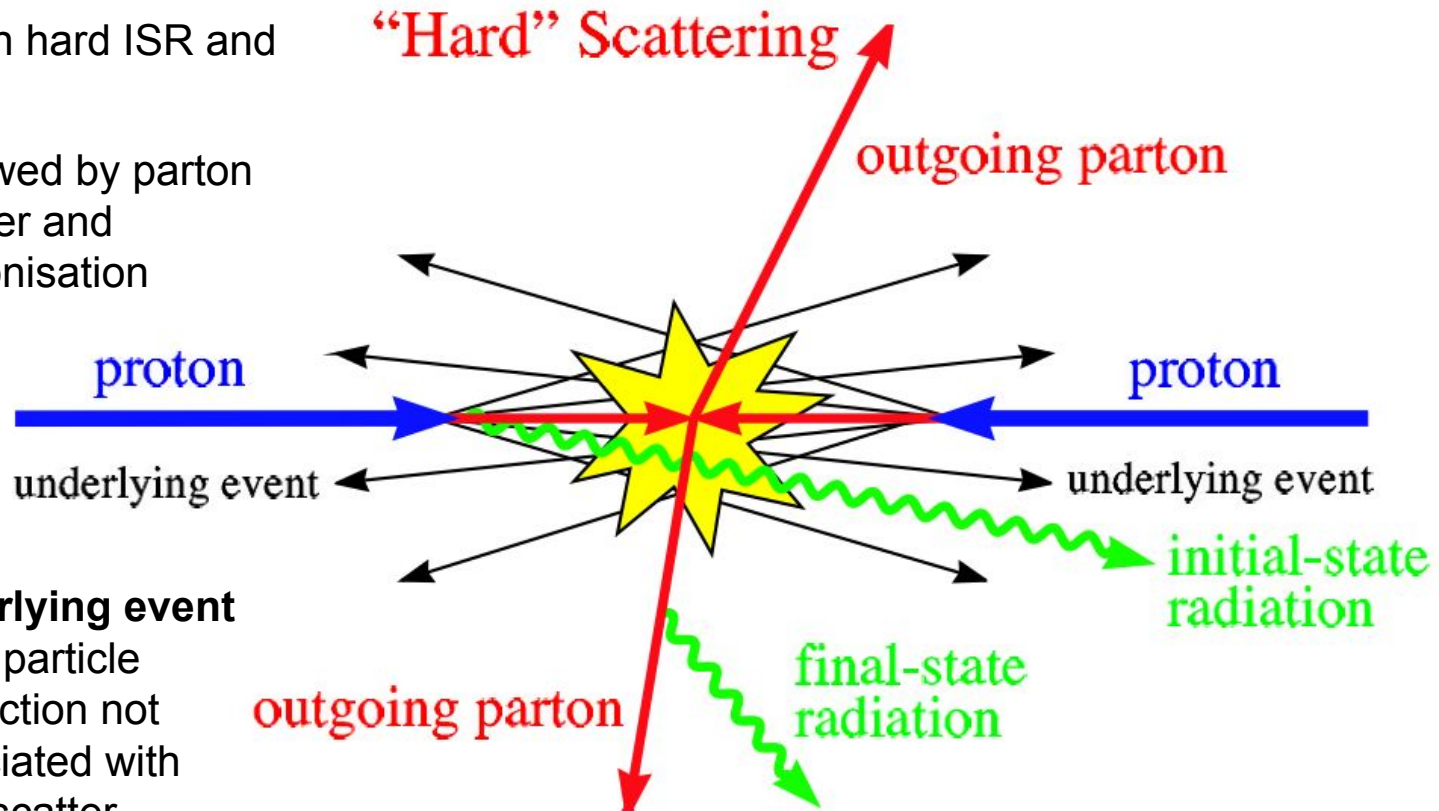
A “typical” LHC collision

- We’re usually interested in hard-scatter (HS) interactions between two partons within the protons
- Add in hard ISR and FSR
- Followed by parton shower and hadronisation



A “typical” LHC collision

- We’re usually interested in hard-scatter (HS) interactions between two partons within the protons
- Add in hard ISR and FSR
- Followed by parton shower and hadronisation

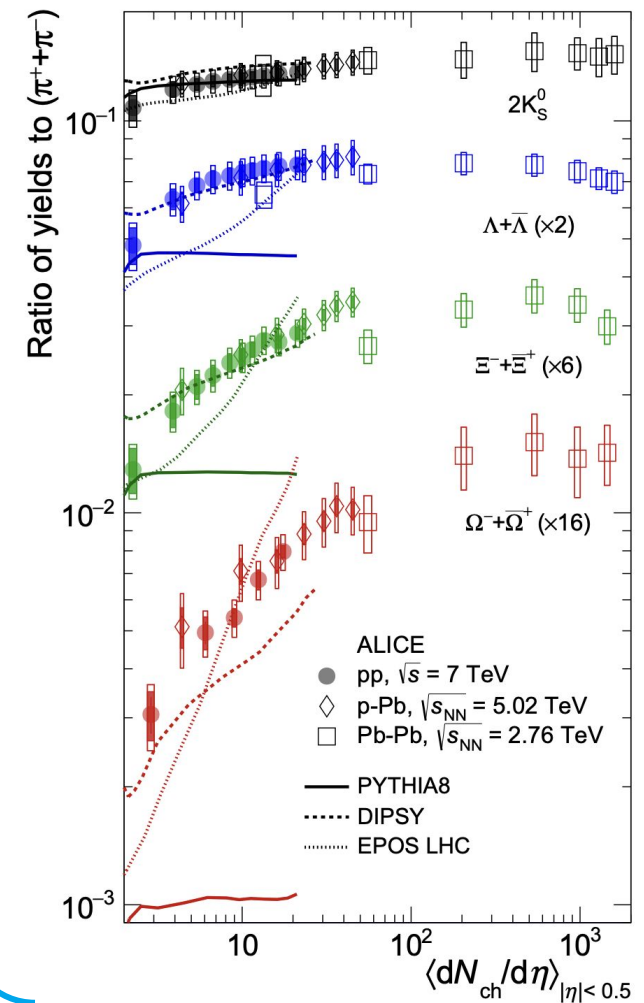


- **Underlying event (UE):** particle production not associated with hard-scatter

- Due to secondary interactions of other constituent partons in the proton → **Multi-parton Interactions (MPI)**
- MPI interactions are not independent → Colour interaction between UE and HS

Analysis motivation

- Measure production of **strange hadrons** in the underlying event
- Typical hadronisation models have parameters that are tuned using collider data of **charged hadrons**
 - Should also consider **neutral hadrons** for full picture of hadronisation in precision measurements
- The mass of the strange quark is close to Λ_{QCD}
 - Probe **interplay between “soft” and “hard” QCD** interactions
- Comparing yields of mesons to baryons allows us to study **colour reconnection** effects
- ALICE Collaboration observed an enhancement of strange to non-strange hadron production with increasing particle multiplicity in pp collisions [[arXiv:1606.07424](https://arxiv.org/abs/1606.07424)]



Measure number of strange baryons and mesons in various regions:

highest- p_T anti- k_T jet with $R = 0.4$ and $|\eta| < 2.1$

Leading Jet

Region most sensitive to hard scatter and hadronisation

Region most sensitive to MPI

$-\pi/3$

$+\pi/3$

Towards

Transverse

Transverse

Away

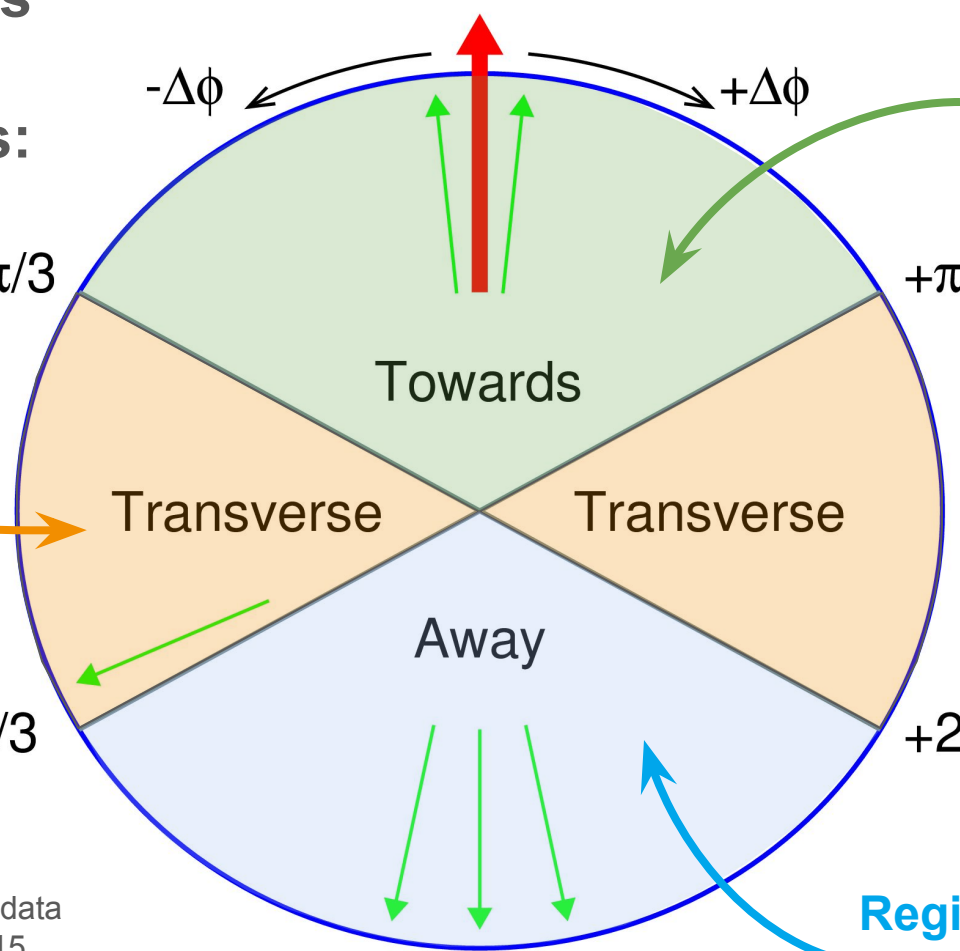
$-2\pi/3$

$+2\pi/3$

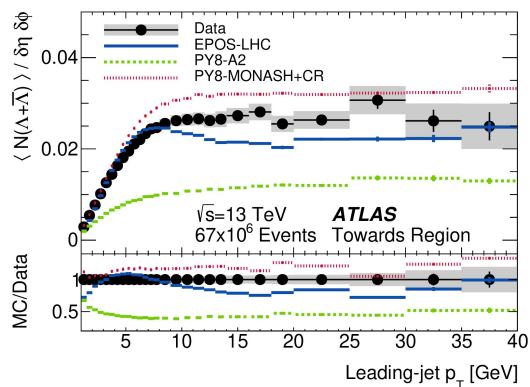
Region most sensitive to hadronic recoil

Measurement performed in minimum-bias very low-pileup data at $\sqrt{s} = 13$ TeV, recorded in 2015

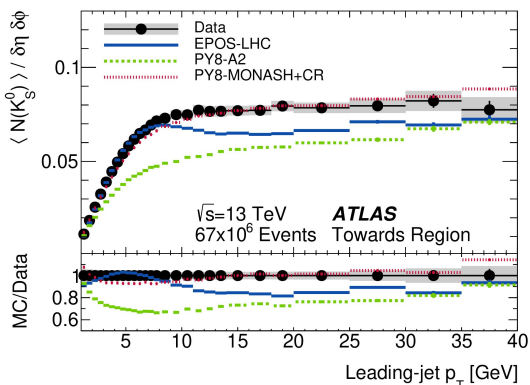
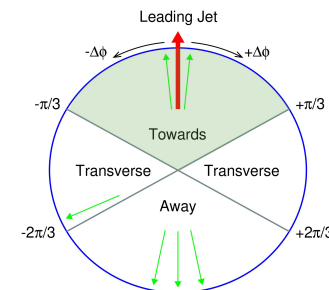
Data are unfolded to particle-level



Event normalised distributions

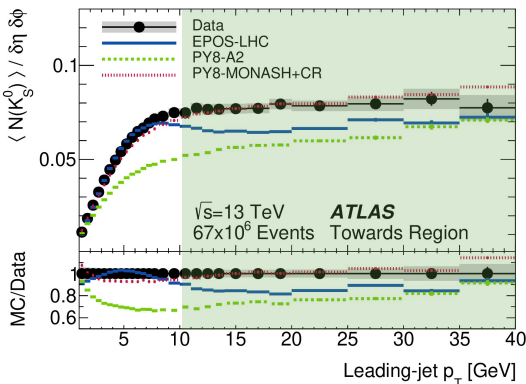
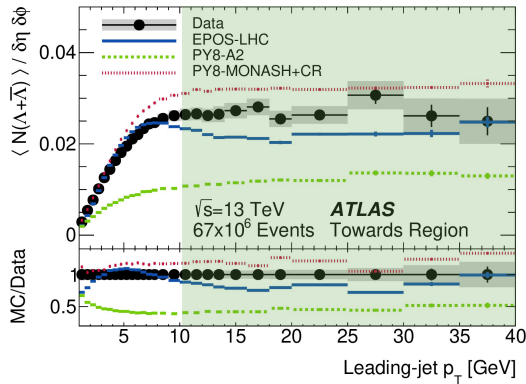


$$\Lambda = uds$$



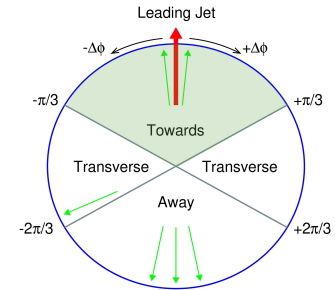
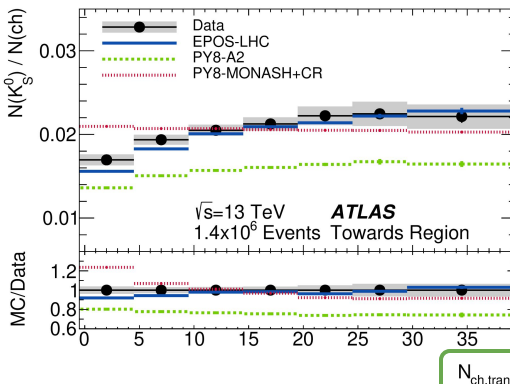
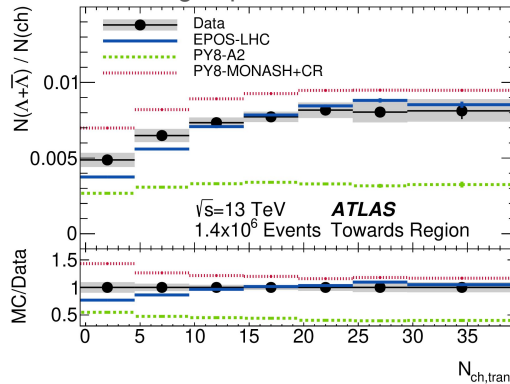
$$K_S^0 = (d\bar{s} - s\bar{d}) / \sqrt{2}$$

Event normalised distributions



Restricted jet- p_T range of 10–40 GeV = “hard regime”

Now normalised to total number of charged particles in the event



Λ

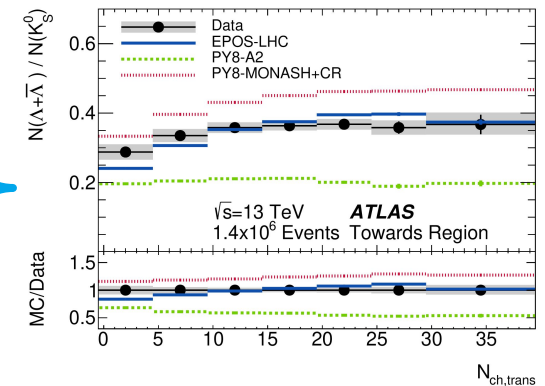
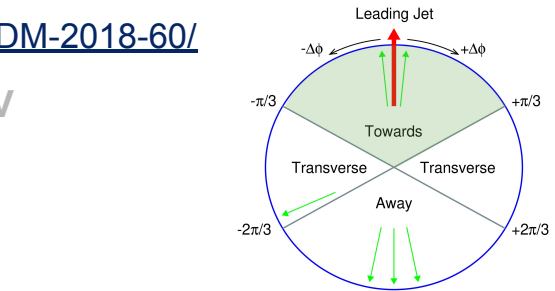
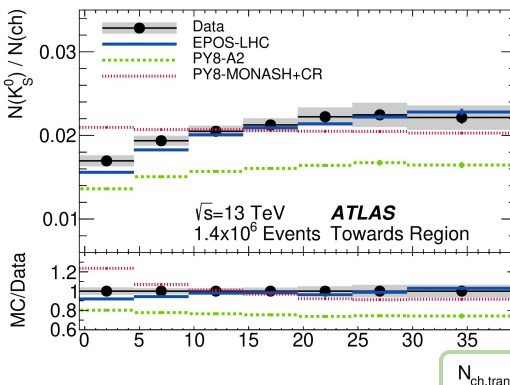
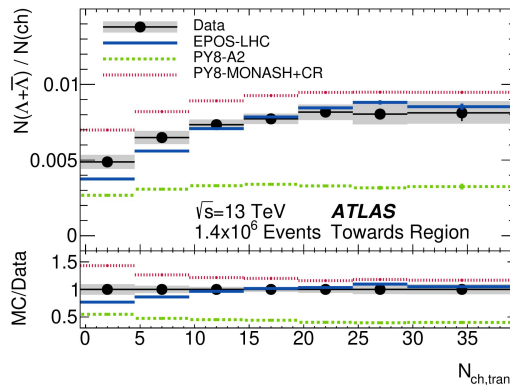
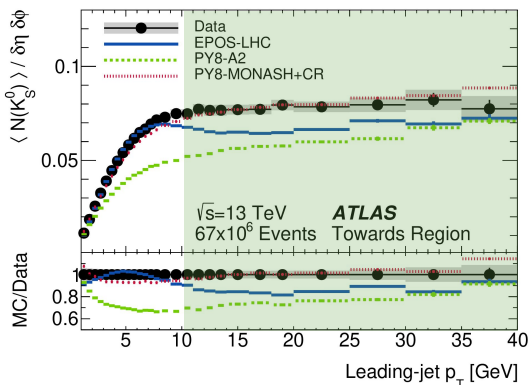
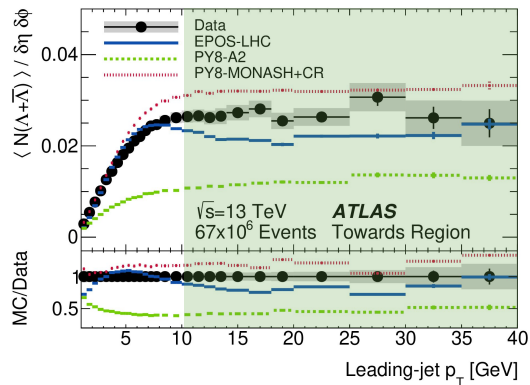
K_S^0

Proxy for MPI in transverse region, i.e. amount of underlying event activity

All plots in all regions at atlas.web.cern.ch/Atlas/GROUPS/PHYSICS/PAPERS/STDM-2018-60/

Event normalised distributions

Restricted jet- p_T range of 10–40 GeV

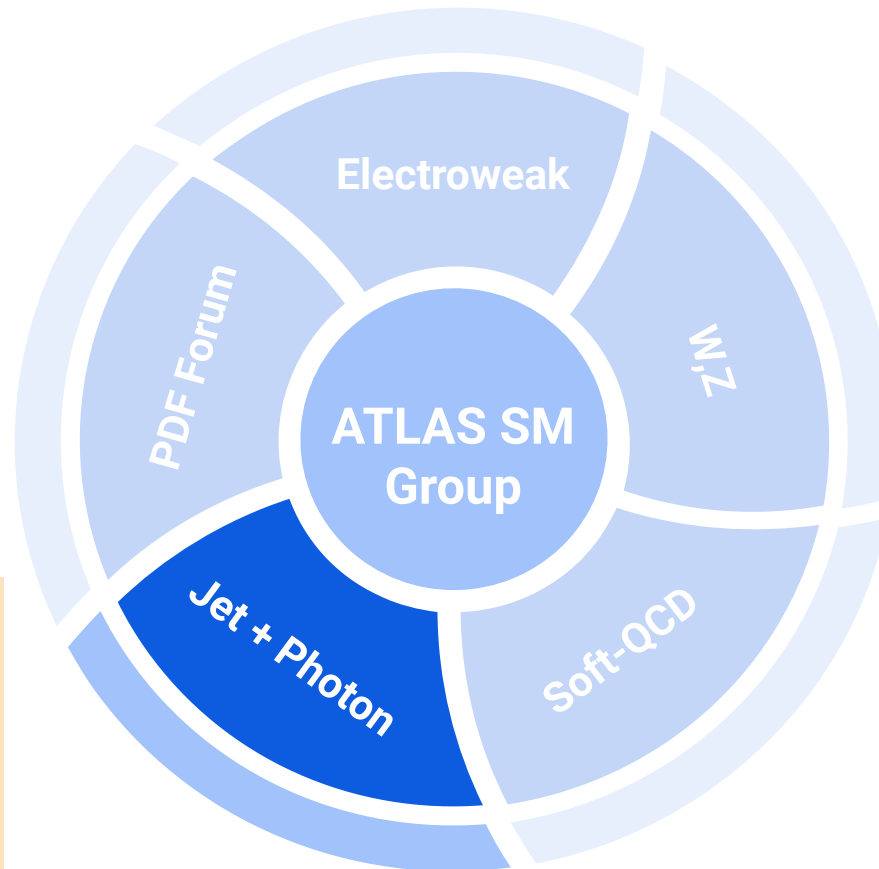


Ratio of strange mesons to baryons largely insensitive to the amount of MPI activity

Proxy for MPI in transverse region, i.e. amount of underlying event activity

ATLAS SM subgroups

SMJetPhotonWorkingGroup

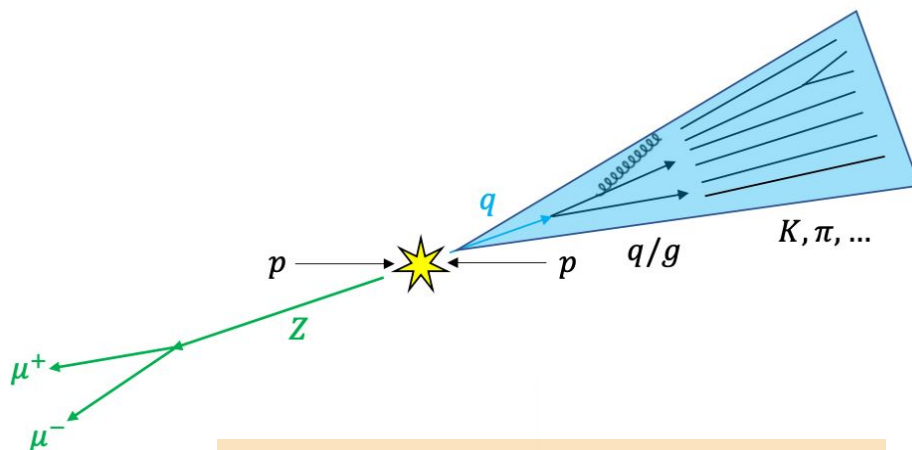


Group interests:

- Jet and prompt photon processes
- Understanding pQCD
- Providing input for PDF fits
- Understanding backgrounds to new physics

Analysis motivation

- Provide precise unfolded measurement of $Z(\rightarrow\mu\mu)+\text{jet}$ process to test perturbative QCD and improve MC predictions
- Common process with low backgrounds that can be measured very precisely
 - Precision probe of the Standard Model
- Full Run 2 analysis at 13 TeV, 139 fb^{-1}



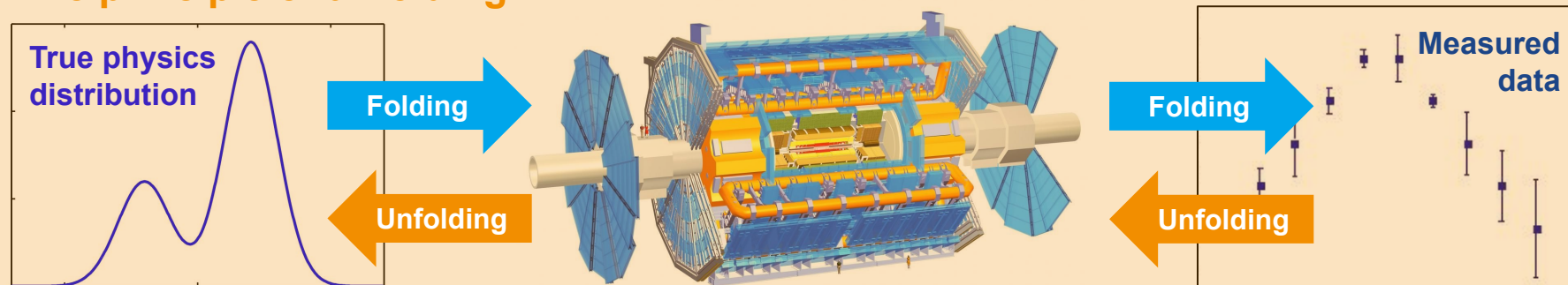
The Drell-Yan process is the standard candle for precision measurements and theory at the LHC

Analysis strategy

- Standard Z+jets selection in boosted regime: $p_T(\mu\mu) > 200\text{ GeV}$
- **Simultaneous measurement of 24 observables** related to the **dimuon and muon kinematics**, **track jet kinematics** and **track jet substructure**
- Unfolding performed via Machine Learning (ML) method “OmniFold”
 - Unlike any previous fiducial differential cross-section measurement, this result is presented as an **unbinned dataset of particle-level events**

- Unfolding aims to remove detector effects from data
 - Our best idea of what the true underlying physics looks like
- Necessary for comparing to other experimental results and theoretical models

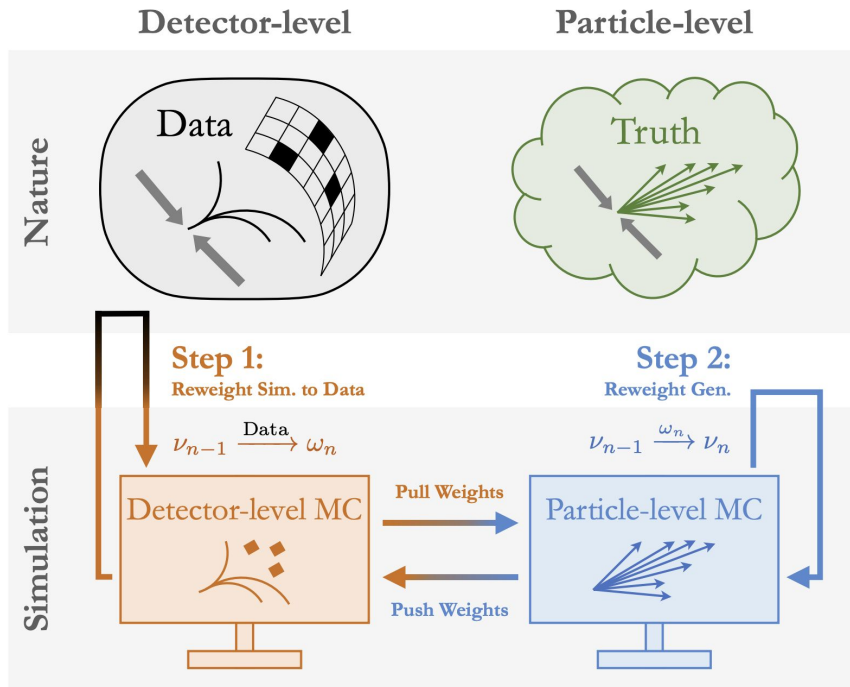
The principle of unfolding:



Unfolding in a “typical” analysis

- Traditional unfolding techniques work with 1D binned data
- Several potential downfalls:
 - Target observables must be specified prior to unfolding
 - The binning is fixed
 - Can only unfold a small number of observables simultaneously
 - Does not consider full phase space and may miss hidden dependencies

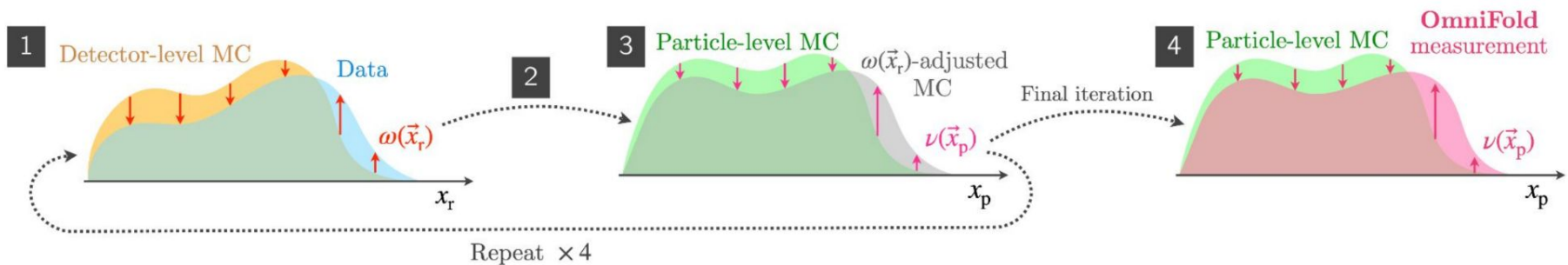
New ML methods aim to address these issues



Multi-stage and iterative process

Series of neural networks are trained to learn a reweighting function that maps particle-level MC distributions to particle-level data distributions

More details on methods in [OmniFold talk from SM workshop 24](#) by Mariel Pettee



Result

- Proof-of-principle application of the OmniFold method to provide an **unbinned, highly-dimensional measurement with full covariance for public use**
- Allowing significant **increased utility** such as adjusting binning and **constructing new observables**
- Entering a new era of **reproducible and re-interpretable results**

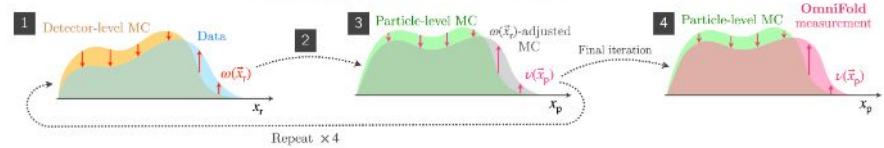
Datasets and code publicly available
gitlab.cern.ch/atlas-physics/public/sm-z-jets-omnifold-2024

README.md

A simultaneous unbinned differential cross section measurement of twenty-four Z+jets kinematic observables with the ATLAS detector

CDS CERN-EP-2024-132 arXiv 2405.20041 DOI 10.5281/zenodo.11507450 launch binder Open In Colab

These notebooks demonstrate how to interact with the unbinned, twenty-four-dimensional ATLAS Z+jets differential cross-section measurement presented in arXiv:2405.20041. This analysis uses OmniFold to mitigate detector effects in data.



Since the data is structured as an unbinned set of events, users can:

- Re-create the differential cross-section distributions (and calculate the associated uncertainties) of the twenty-four measured input observables with a **flexible choice of binnings** (see Fig. 1 below)
- **Modify the measured phase space on-the-fly** (see Fig. 2a & 2b below)
- **Measure new observables** or quantities constructed as a function of the input observables (see Fig. 2 below)

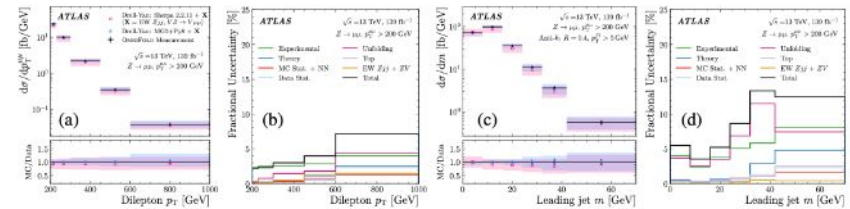


Figure 1: Measured differential cross sections compared with particle-level predictions from SHERPA and MADGRAPH for two of the 24 directly measured observables: (a) p_T^H with its (b) associated uncertainty breakdown; and, (c) m_{j1} with its (d) associated uncertainty breakdown. For display purposes, binned (marginal) distributions are shown, though the measurement itself is unbinned and 24-dimensional.

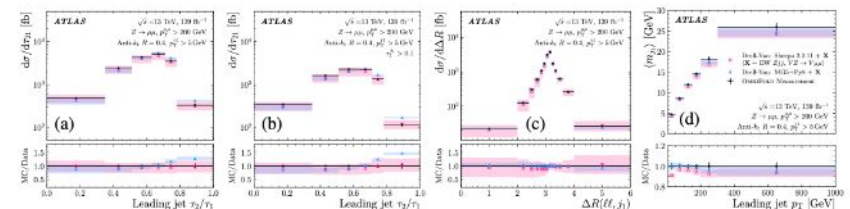


Figure 2: Four measurements of quantities constructed from several of the 24 input observables, along with particle-level predictions from SHERPA and MADGRAPH: the jet substructure observable $\tau_{21}^{J1} = \tau_2^{J1}/\tau_1^{J1}$ in (a) the reduced region defined by $\tau_1^{J1} > 0.1$; (b) ΔR between the dilepton system and the leading jet; and, (c) the average m_{j1} as a function of p_T^{J1} .

Make your own measurement

zenodo.org/records/11507450

Published June 6, 2024 | Version v1

Dataset 

ATLAS OmniFold 24-Dimensional Z+jets Open Data

ATLAS Collaboration 

These datasets contain the unbinned, twenty-four-dimensional ATLAS Z+jets differential cross-section measurement presented in [CERN-EP-2024-132](#). The measurements are presented as Pandas DataFrames in HDF5 format, and they are accompanied by MC predictions formatted as Numpy arrays. Measurements are provided both for "pseudo-data", i.e. a validation MC sample with truth- and reco-level quantities that has been reweighted to match data, as well as real data.

Important: Before using this data, please consult the [documentation & example notebooks](#).

The signal process is inclusive $Z \rightarrow \mu\mu$ production with a fiducial region defined in the boosted regime: $p_{T}^{\mu\mu} > 200$ GeV.

In total, 24 Z+jets kinematic observables are measured:

- p_{T} , η , and ϕ of each of the two muons (6 observables)
- The p_{T} and rapidity of the dimuon system: $p_{T}^{\mu\mu}$, $y^{\mu\mu}$ (2 observables)
- The 4-momenta (p_{T} , y , ϕ , m) of the two leading charged particle jets (8 observables)
- The number of (charged) constituents and n -subjettiness quantities $\tau_{1,2,3}$ for each of the same two jets (8 observables)

The dimuon system p_{T} and y can be obtained from the muon kinematics, but they are included for convenience. The observables are labeled by 1 and 2 for leading and subleading in p_{T} , respectively.

Files

files.zip 

 files.zip 

178

 VIEWS

66

 DOWNLOADS

 Show more details

Versions

Version v1

Jun 6, 2024

[10.5281/zenodo.11507450](https://doi.org/10.5281/zenodo.11507450)

Cite all versions? You can cite all versions by using the DOI [10.5281/zenodo.11507449](https://doi.org/10.5281/zenodo.11507449). This DOI represents all versions, and will always resolve to the latest one. [Read more](#).

External resources

Indexed in

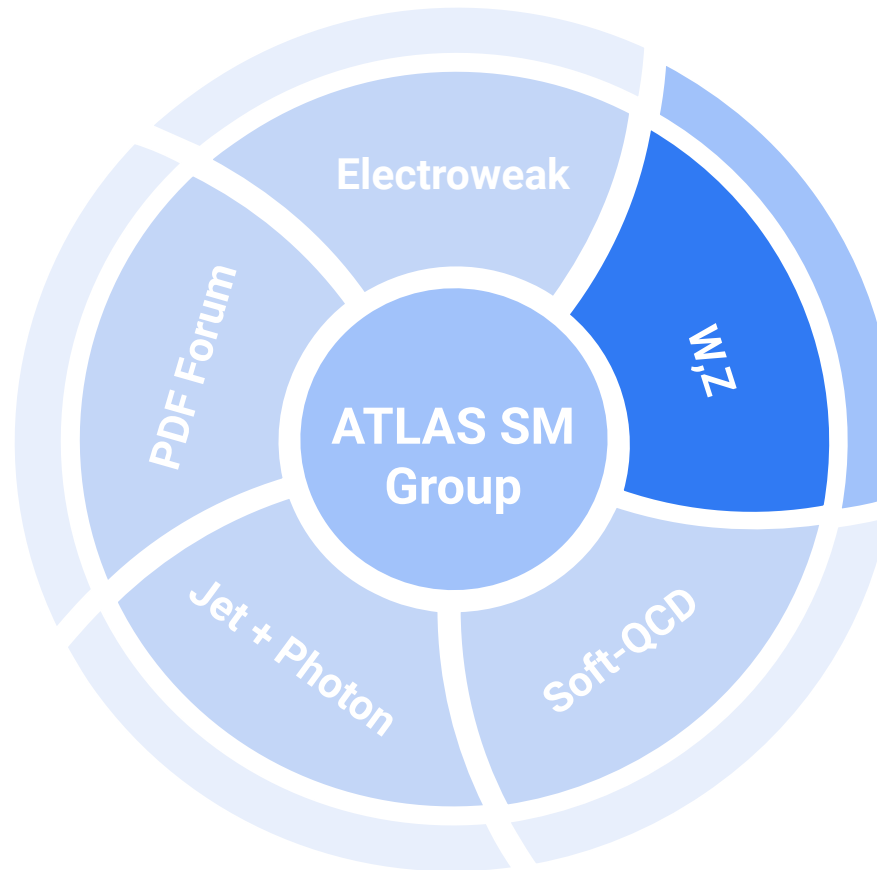


Communities

 The ATLAS Experiment at CERN

ATLAS SM subgroups

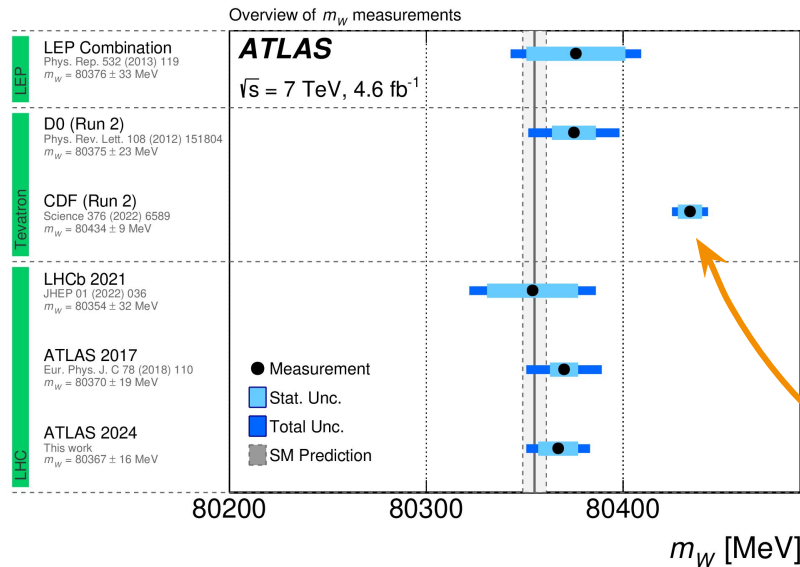
SMWZSignaturesWorkingGroup



Group interests:

- W and Z production
- Off-peak Drell-Yan (also in association with light and heavy flavour jets)
- Inclusive lepton production at low p_T
- Precision measurements of SM parameters

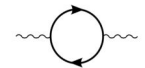
Analysis motivation



- Parameters of SM electroweak sector tightly linked to other fundamental parameters

$$m_W = \left(\frac{\pi \alpha_{EM}}{\sqrt{2} G_F} \right)^{1/2} \frac{\sqrt{1 + \Delta r}}{\sin \theta_W}$$

Radiative corrections Δr with largest contributions from m_t^2 and $\log(m_H)$



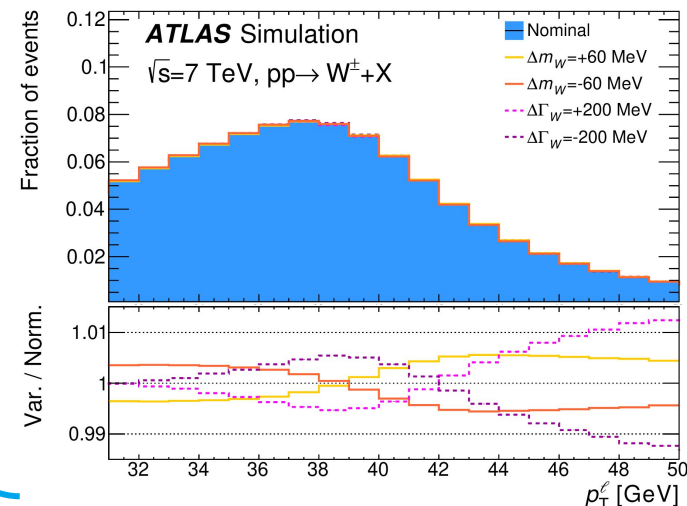
- New physics can alter m_W through loop corrections

Hot topic due to surprise CDF 2022 result

- Re-analysis of 7 TeV data from Run 1, using **improved analysis techniques**
- Also benefit from **progress in global PDF fits** and theoretical calculations
- W-width, Γ_W , never measured before at the LHC**
 - Value precisely predicted by the SM
 - Light new physics (mass $< m_W$) that couples to the W-boson would alter Γ_W from SM value

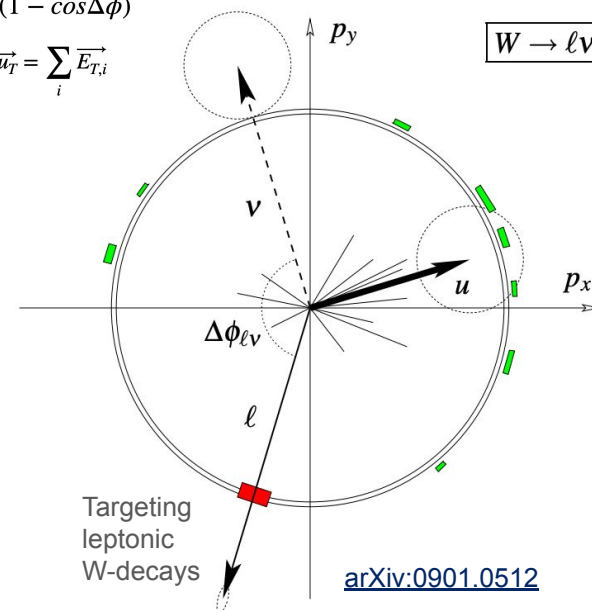
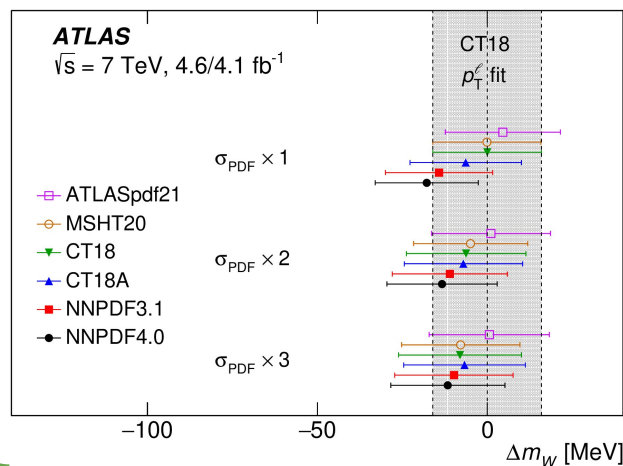
Analysis strategy

- Kinematic distributions sensitive to changes in W-mass and width
- Previous analysis χ^2 fit with stat. uncertainties only
 - systematic uncertainties added afterwards
- Updated analysis uses profile likelihood fitting
 - systematic uncertainties included as nuisance parameters
- Updated QCD background estimation
- Analysis thoroughly investigated impact of PDF choice and uncertainty on the result



$$m_T = \sqrt{2p_T^l p_T^{miss}(1 - \cos\Delta\phi)}$$

$$\vec{p}_T^v = -\vec{p}_T^l - \vec{u}_T \quad \vec{u}_T = \sum_i \vec{E}_{T,i}$$



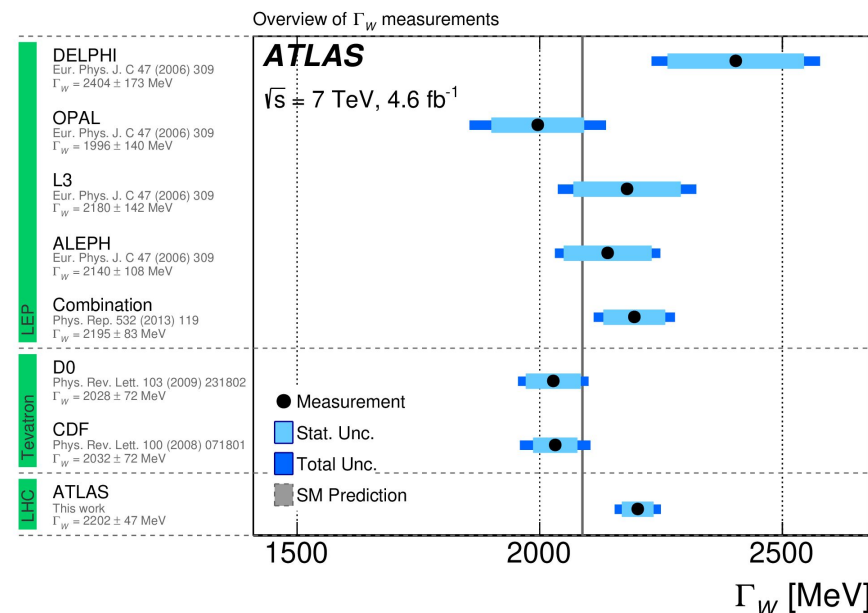
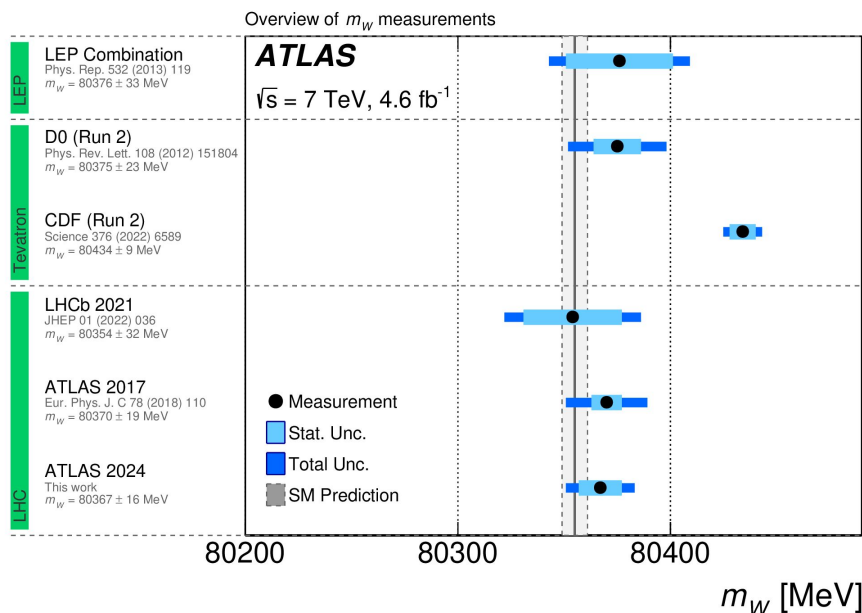
arXiv:0901.0512

Results

- Separate fits are performed to the $p_T(\ell)$ and m_T distributions
- m_W : Systematic uncertainties dominated by PDF uncertainties, missing higher-order EW corrections, and lepton calibration uncertainties
- Γ_W : Dominant systematic uncertainties are due to the parton shower modelling for $p_T(\ell)$, and lepton and recoil performance for m_T , respectively
- Currently most precise single measurement of Γ_W

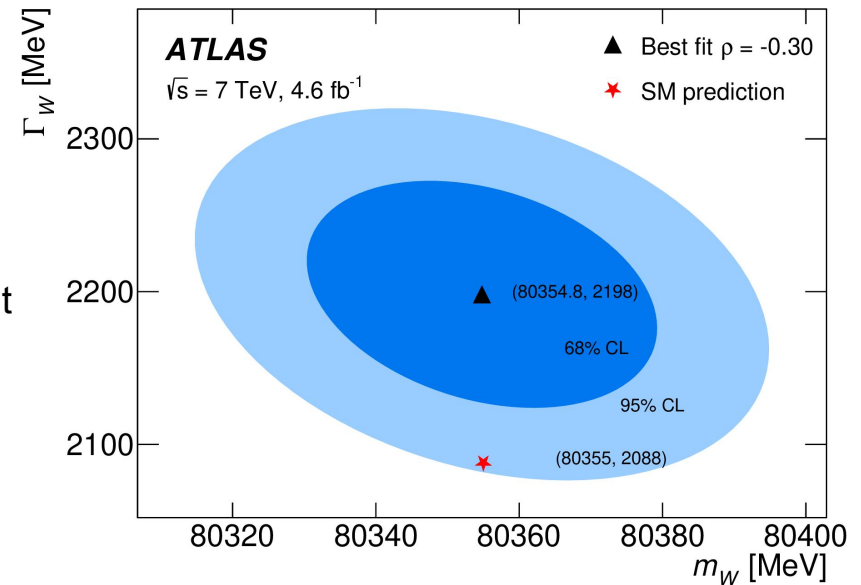
$$m_W = 80366.5 \pm 9.8 \text{ (stat.)} \pm 12.5 \text{ (syst.) MeV} = 80366.5 \pm 15.9 \text{ MeV}$$

$$\Gamma_W = 2202 \pm 32 \text{ (stat.)} \pm 34 \text{ (syst.) MeV} = 2202 \pm 47 \text{ MeV}$$



Combined fit

- Individual fits of m_W and Γ_W assume the other value is fixed to global EW fit result
- Observed dependence of the two observables:
 - $\Delta m_W = -0.06 \Delta \Gamma_W$
 - $\Delta \Gamma_W = -1.25 \Delta m_W$
- Further test interdependence with simultaneous fit of both observables:
 - $m_W = 80354.8 \pm 16.1 \text{ MeV}$
 - $\Gamma_W = 2198 \pm 49 \text{ MeV}$
 - -30% correlation

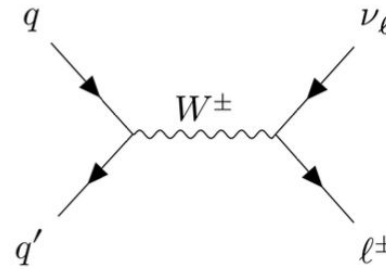


Next week: LHC Seminar - High-precision measurement of the W boson mass at CMS indico.cern.ch/event/1441575/

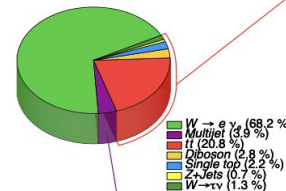
Also this year: Precise measurements of W- and Z-boson transverse momentum spectra in special low pileup runs at $\sqrt{s} = 5.02 \text{ TeV}$ and 13 TeV [\[arXiv:2404.06204\]](https://arxiv.org/abs/2404.06204) (submitted to EPJC)

Differential W cross section at high transverse mass

- Charged current Drell-Yan process
 - Benchmark process at the LHC
 - High statistics available
 - Measure cross-section differentially in the transverse mass $m_T(W)$ and double-differentially in $m_T(W)$ and $\eta(\ell)$
- Applications
 - Constraints on PDFs
 - Sensitivity to the running electroweak coupling
 - Test of lepton universality
 - EFT interpretation

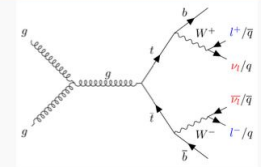


ATLAS Internal
high m_T^W, e^+



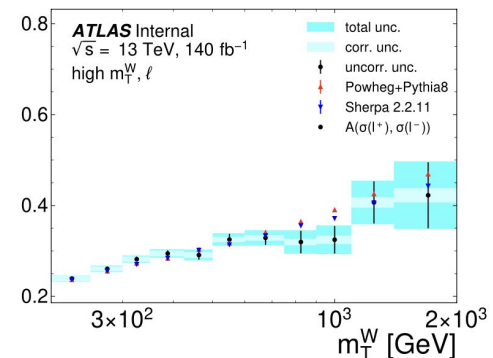
Background modeled with MC

- $t\bar{t}$
- $Z \rightarrow \ell\ell$
- Single top
- Diboson
- $W \rightarrow \tau\nu$



Multijet

- Muons from heavy flavour decays
- Jet fakes an electron in the detector
- Estimated via data-driven matrix method



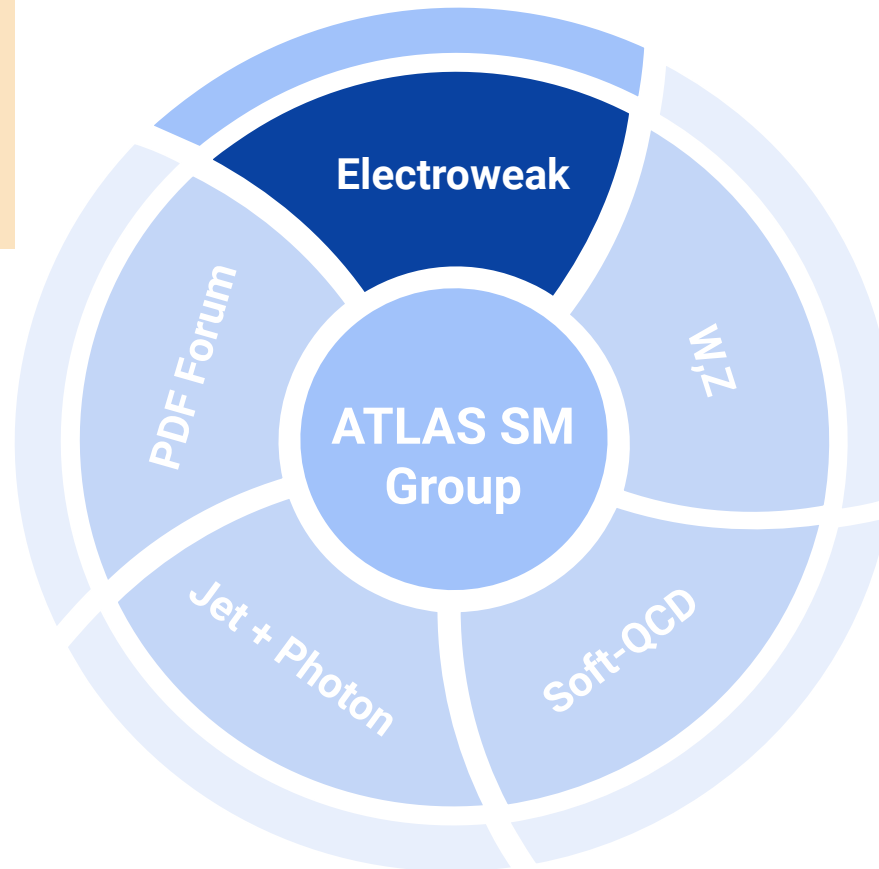
For many more details, see [talk by Tim Beumker](#)

ATLAS SM subgroups

Group interests:

- Diboson production and interactions
- Vector-boson scattering and fusion (VBS and VBF)
- Triboson physics

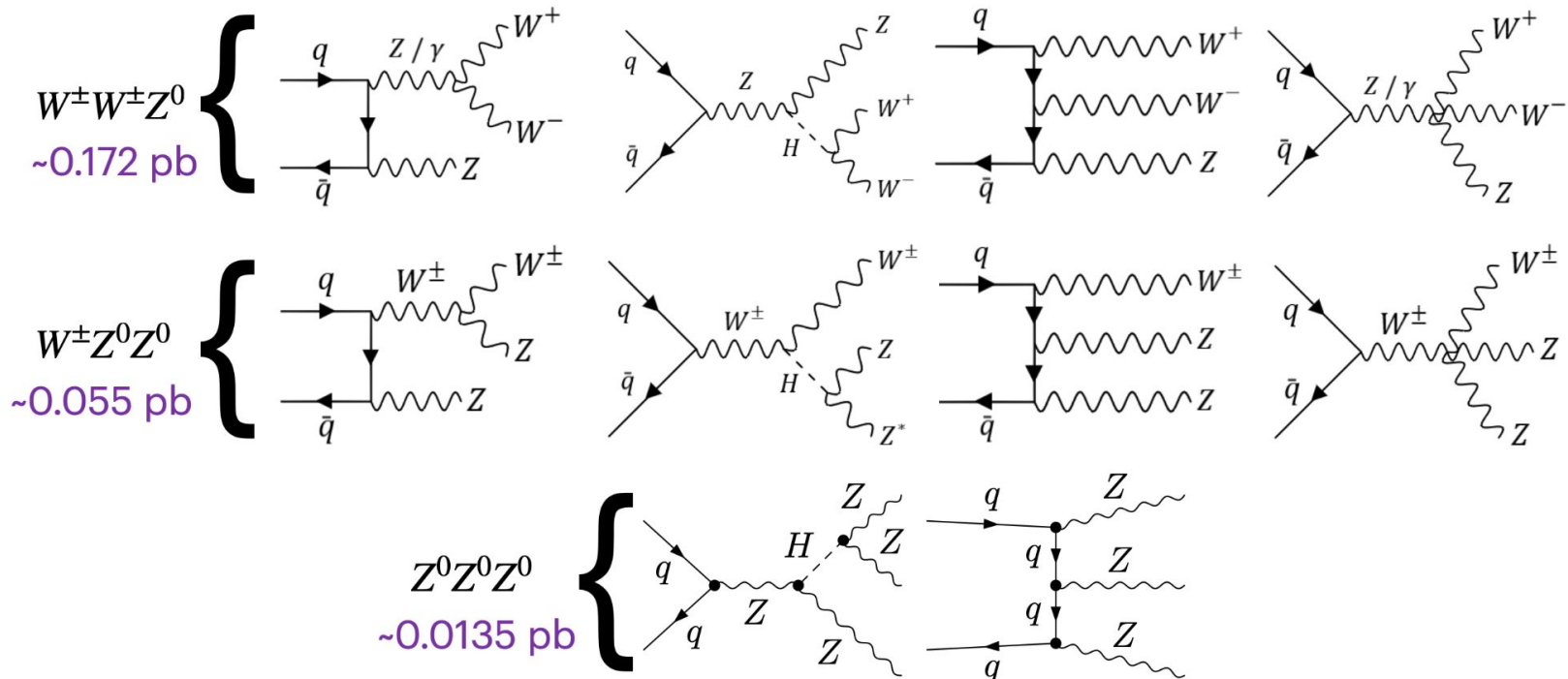
ElectroweakWorkingGroup



See also: Symposium [talk on SM diboson measurements](#) by Frank Siegert

Analysis motivation

- **Triboson processes** are some of the **rarest SM processes** accessible at the LHC
 - $Z\gamma\gamma$, $W\gamma$, $WZ\gamma$ and WWW observed by ATLAS so far, evidence for WVZ
- Complement other multiboson probes of **anomalous vector boson couplings**
- Utilise full Run 2 dataset and improve on previous ATLAS WVZ analysis [[PLB 798 \(2019\) 134913](#)]



Analysis strategy

- Targeting a combination of semi- and fully-leptonic final states

$3\ell + \text{jets}$

$WZ \rightarrow qq$

$W \rightarrow \ell\nu$

$Z \rightarrow \ell\ell$

$$\Gamma_i/\Gamma_{total}(WWZ) = 1.01 \%$$

$$\Gamma_i/\Gamma_{total}(WZZ) = 1.05 \%$$

4ℓ

$W \rightarrow \ell\nu$

$W \rightarrow \ell\nu$

$Z \rightarrow \ell\ell$

$$\Gamma_i/\Gamma_{total}(WWZ) = 0.32 \%$$

$\geq 5\ell$

$WZ \rightarrow \ell\nu\ell\ell$

$Z \rightarrow \ell\ell$

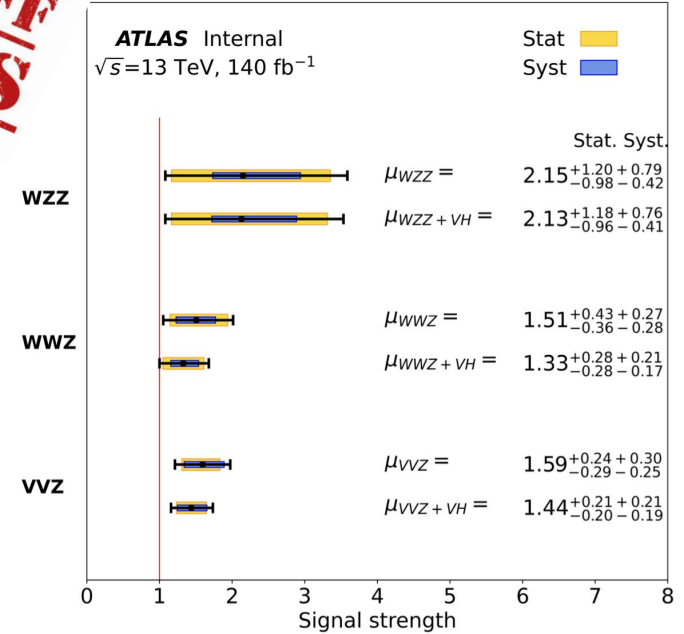
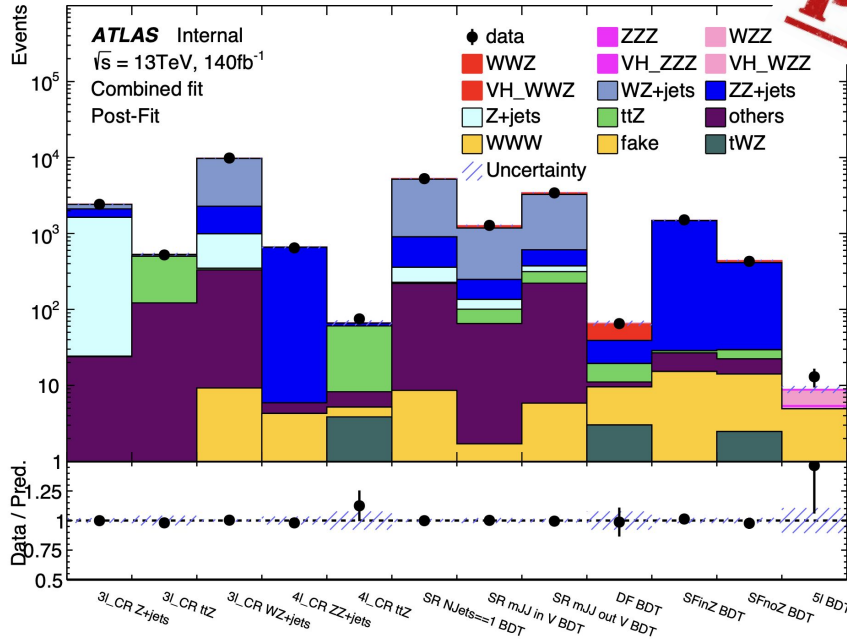
$Z \rightarrow \ell\ell$

$$\Gamma_i/\Gamma_{total}(WZZ) = 0.32 \%$$

$$\Gamma_i/\Gamma_{total}(ZZZ) = 0.11 \%$$

- Multivariate analysis (MVA) to enhance signal sensitivity
 - Profile likelihood fit to BDT distributions in each signal region
- Signal modelled with Sherpa 2.2.2 at NLO QCD accuracy
- Constrain New Physics with an aQGC SMEFT interpretation (EFT signals modelled with MadGraph)
- Dominant backgrounds from diboson production and ttZ

Unblinded post-fit event yields



Fit results:

- ★ First observation of VVZ: 6.4σ observed (4.7σ expected)
- ★ First evidence of WWZ: 4.4σ observed (3.6σ expected)

ATLAS is consistently observing divergences from current SM predictions for massive triboson production

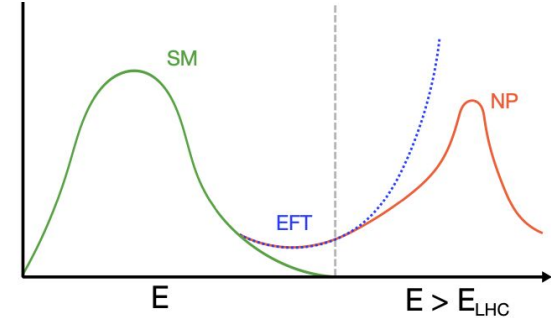
→ WWW observation [[PRL 129 \(2022\) 061803](#)] also measured high signal strengths

EFT interpretation

- Parametrise anomalous vector boson couplings through SM Effective Field Theory (SMEFT) framework
 - Quartic gauge boson couplings sensitive to dim-8 operators
- EFT model only available at LO
 - K-factor correction applied to account for large NLO enhancements to triboson production
- Retrain BDTs with expanded definitions of “signal” now including a range of EFT signal strengths
- Profile likelihood fit it to a BDT output which targets EFT like events
- Clipping scans performed to give unitarised limits:

Coefficient	Expected limit [TeV ⁻⁴]	Exp. E _C [TeV]	Observed limit [TeV ⁻⁴]	Obs. E _C [TeV]
f _{M2} /Λ ⁴	[-18, 17]	1.2	[-19, 19]	1.2
f _{M3} /Λ ⁴	[-28, 29]	1.5	[-28, 29]	1.5
f _{M5} /Λ ⁴	[-14, 14]	1.6	[-12, 12]	1.7
f _{M5} /Λ ⁴	[-11, 11]	2.1	[-9.1, 9.3]	2.2

$$\mathcal{L}_{SMEFT} = \mathcal{L}_{SM} + \mathcal{L}^{(5)} + \mathcal{L}^{(6)} + \mathcal{L}^{(7)} + \dots, \quad \mathcal{L}^{(d)} = \sum_{i=1}^{n_d} \frac{f_i^{(d)}}{\Lambda^{d-4}} \mathcal{O}_i^{(d)} \quad \text{for } d > 4,$$



	WWWW	WWZZ	WW γ Z	WW $\gamma\gamma$
$\mathcal{O}_{S,0}, \mathcal{O}_{S,1}$	✓	✓		
$\mathcal{O}_{M,0}, \mathcal{O}_{M,1}, \mathcal{O}_{M,6}, \mathcal{O}_{M,7}$	✓	✓	✓	✓
$\mathcal{O}_{M,2}, \mathcal{O}_{M,3}, \mathcal{O}_{M,4}, \mathcal{O}_{M,5}$		✓	✓	✓
$\mathcal{O}_{T,0}, \mathcal{O}_{T,1}, \mathcal{O}_{T,2}$	✓	✓	✓	✓
$\mathcal{O}_{T,5}, \mathcal{O}_{T,6}, \mathcal{O}_{T,7}$		✓	✓	✓
$\mathcal{O}_{T,8}, \mathcal{O}_{T,9}$				✓

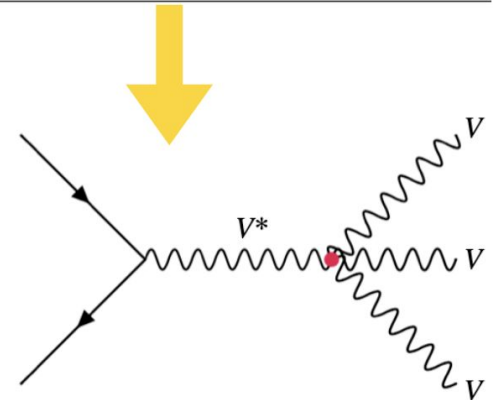
$$\mathcal{O}_{M,2} = [B_{\mu\nu} B^{\mu\nu}] \times [(D_\beta \Phi)^\dagger D^\beta \Phi]$$

$$\mathcal{O}_{M,3} = [B_{\mu\nu} B^{\nu\beta}] \times [(D_\beta \Phi)^\dagger D^\mu \Phi]$$

$$\mathcal{O}_{M,4} = [(D_\mu \Phi)^\dagger \widehat{W}_{\beta\nu} D^\mu \Phi] \times B^{\beta\nu}$$

$$\mathcal{O}_{M,5} = [(D_\mu \Phi)^\dagger \widehat{W}_{\beta\nu} D^\nu \Phi] \times B^{\beta\mu} + \text{h.c.}$$

1604.03555



ATLAS SM Workshop 2024

indico.cern.ch/event/1397505/

The **2024 ATLAS Standard Model workshop** took place **last week** at the **Jožef Stefan Institute** in **Ljubljana, Slovenia**

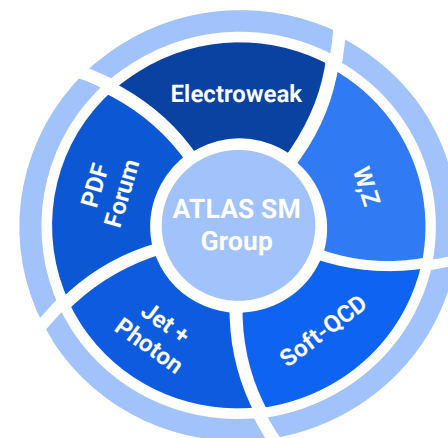
Focus was on the **future of SM measurements** within ATLAS
New analyses, **unexplored processes**, **new techniques**

Highlighting importance of combined performance (CP) and physics modelling (PMG) work in reducing systematic uncertainties



Summary

- The LHC is competing with previous machines in electroweak precision
 - Facilitated by large datasets, detailed understanding of the detectors, dedicated reconstruction techniques and state-of-the-art theory predictions
 - Improved measurements of key electroweak parameters
- SM group also providing precision measurements of both soft and hard QCD phenomena
 - Vital for improvements in modelling
- The LHC has not found a clear signal of BSM physics → new physics will most likely be found through deviations in precision measurements
 - It's an exciting time to do Standard Model physics!
 - Lots of room for new innovation and ideas



NEW: Comprehensive summary of Electroweak, QCD and flavour physics studies with ATLAS data from Run 2 of the LHC
[arXiv:2404.06829](https://arxiv.org/abs/2404.06829) (Submitted to Physics Reports)

Latest updates from the PDF Forum in backup

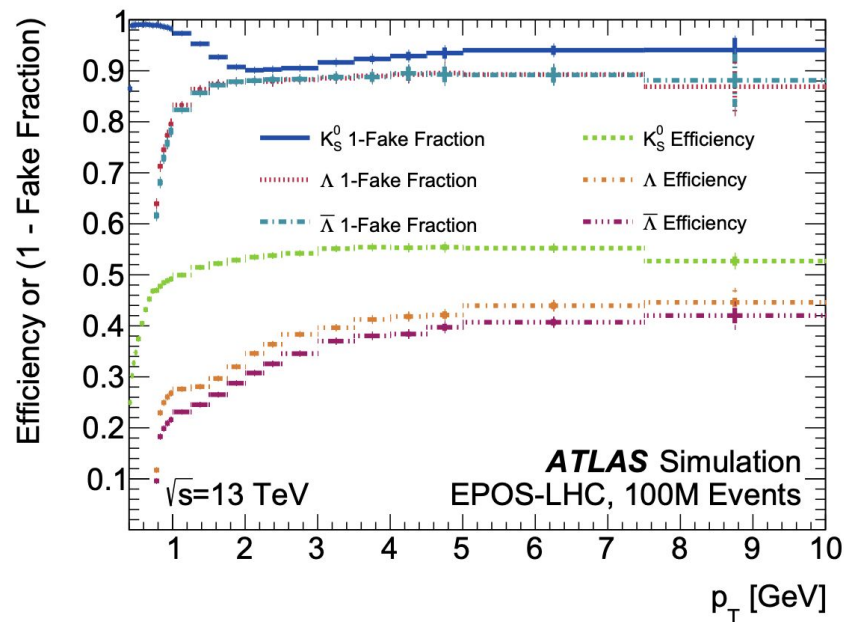
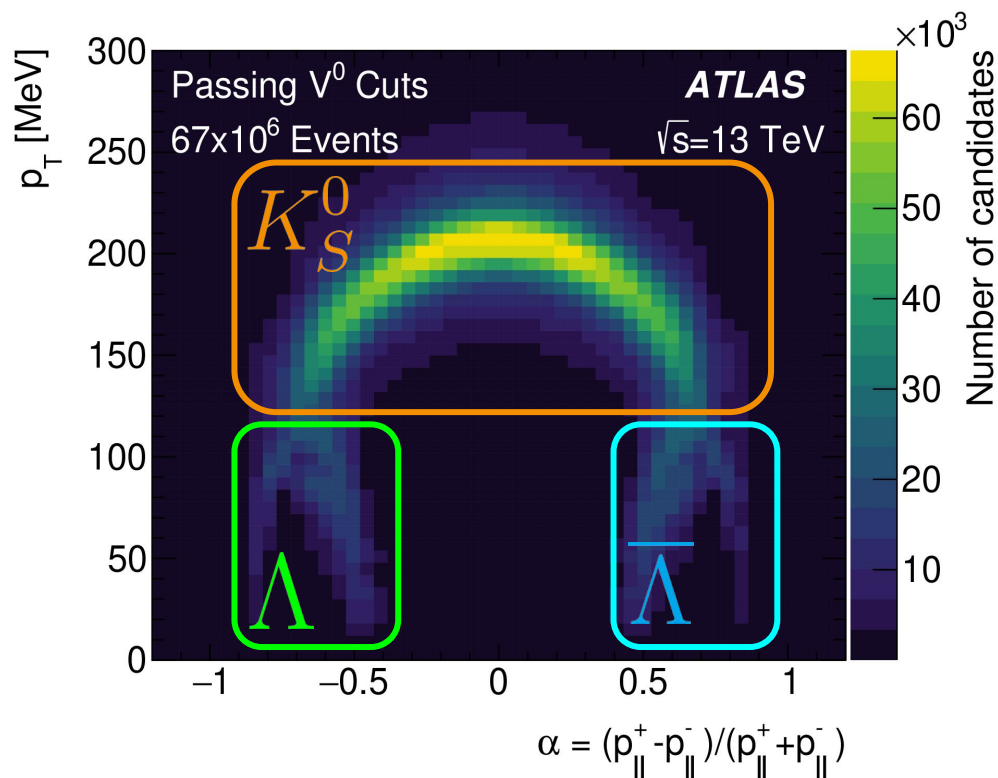
Backup

Highlights from the PDF Forum

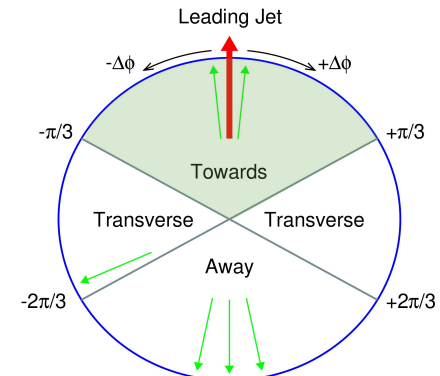
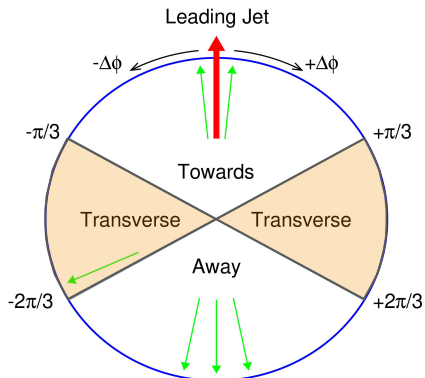
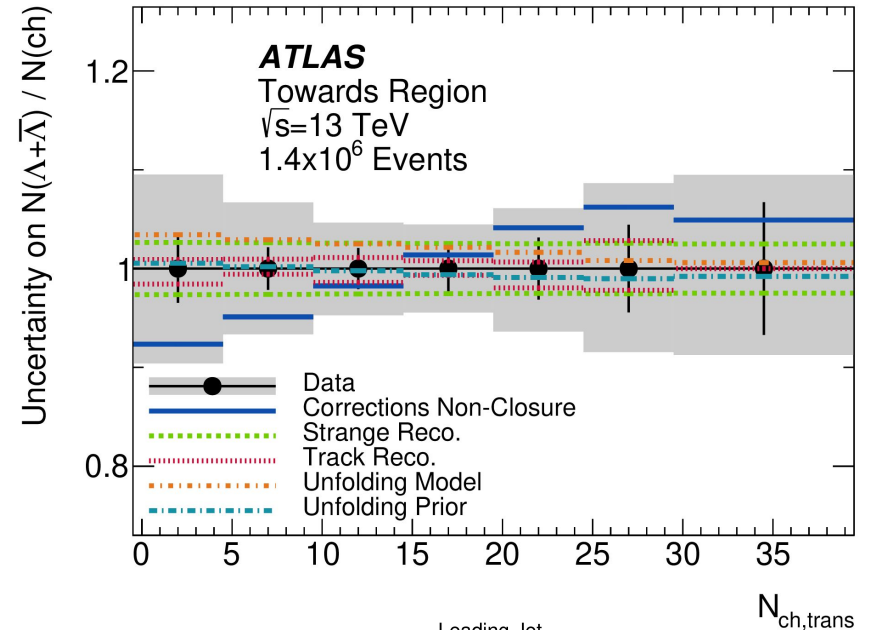
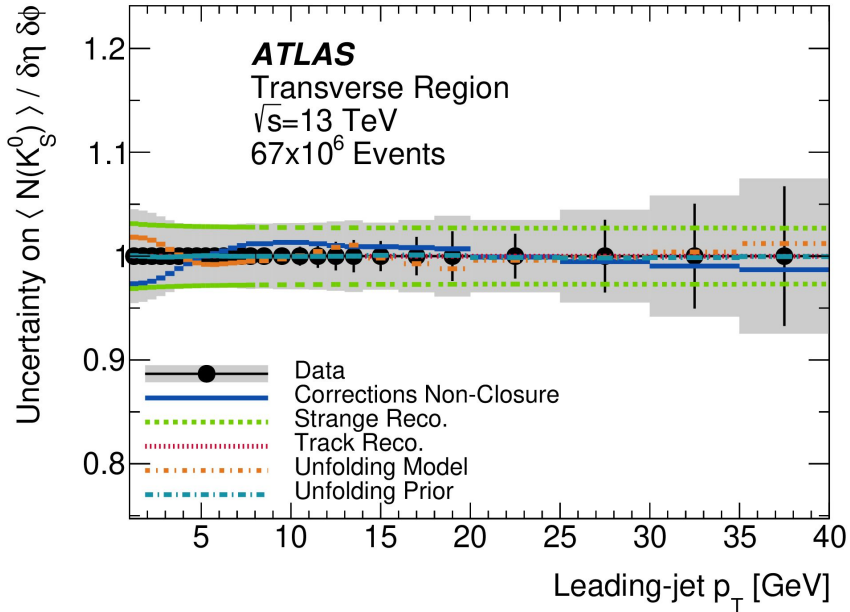
- **Current priority = Identifying ATLAS measurements that could inform update to ATLASpdf21 fit**
 - Most will come from full Run 2 measurements wrapping up
 - Input requires both experimental data and NNLO predictions (either directly at NNLO or NLO + k-factors)
- **JETS:** Three measurements: 8 TeV inclusive, 13 TeV inclusive (15+16), 13 dijet
 - Systematic correlations between datasets needed to be clarified to use several at once
 - Prelim. fits performed for all three simultaneously
 - Inclusion of new full Run 2 13 TeV inclusive jet data (replacing 15+16) in progress
- **TTBAR:** Full Run 3 TeV ttbar
 - In progress, team working on systematic uncertainties
 - Analysers working closely with the PDF forum (encouraged universally for PDF-sensitive measurements!), aware of need for full info on systematic correlations and dialogue with theoreticians for NNLO predications & interpolation grids
 - Sensitivity to m_{top} and $\alpha_s(M_Z)$ also under investigation
- **COMPLETE OR IN THE PIPELINE...** but predictions are missing, not available at NNLO or insufficiently precise, e.g.:
 - 13 TeV $W \pm D^*$ ([arXiv:2302.00336](https://arxiv.org/abs/2302.00336)), 13 TeV $W+c$
 - 13 TeV direct photon ([arXiv:2302.00510](https://arxiv.org/abs/2302.00510))
 - 13 TeV $W+jets$ ([Glance](#))
- ... or more delicate theoretical treatment required, e.g.:
 - Low-x resummation for 7 TeV W,Z (e.g. [arXiv:2209.13535](https://arxiv.org/abs/2209.13535))
- Requires close collaboration with theorists

Thanks to Eimear Conroy (Oxford) for updates

Strange hadron reconstruction



Systematic uncertainties



24 measured event observables:

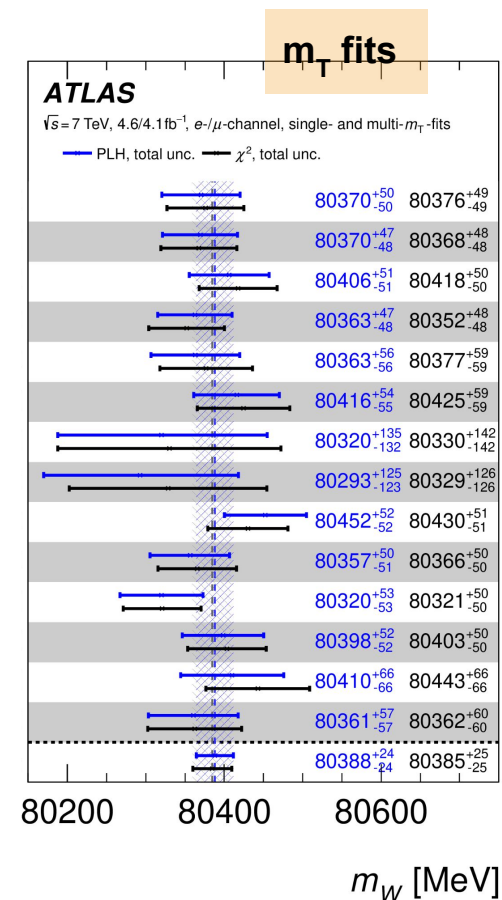
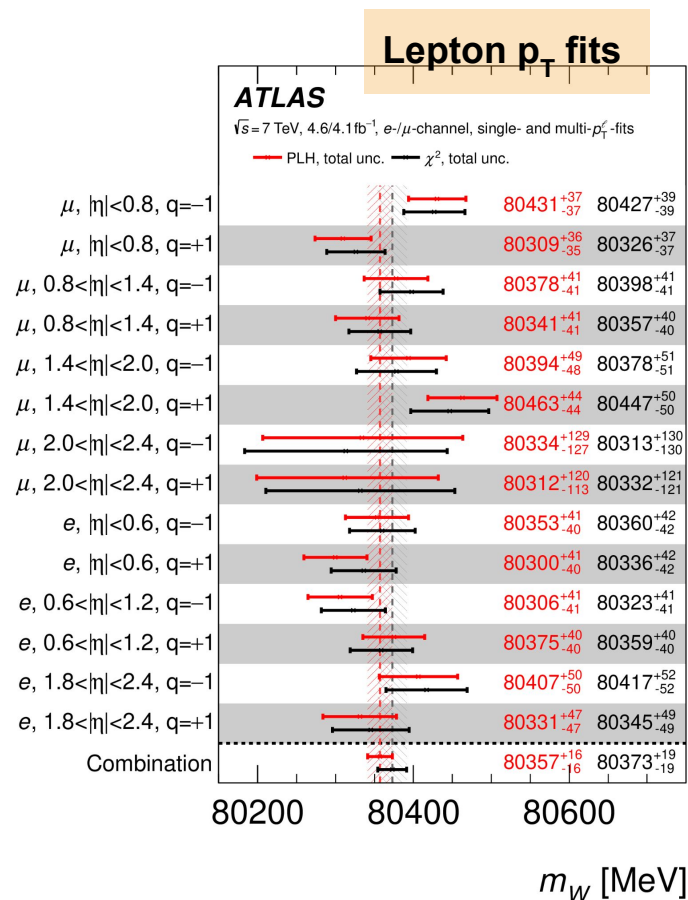
- Dimuon system: $p_{T\mu\mu}$ and $y_{\mu\mu}$
- Single muon kinematics: $p_{T\mu}$, η_{μ} , ϕ_{μ}
- Jet kinematics: defined by p_{Tj} , y_j , ϕ_j , m_j
- charged particle multiplicities n_{jch}
- Jet substructure probes: N -subjettiness quantities τ_{j1} , τ_{j2} , τ_{j3} , τ_{j4}

Event selection:

- two prompt “dressed” muons with opposite-sign
- Muon $p_T > 25$ GeV and $|\eta| < 2.5$
- $m_{\mu\mu} \in (81, 101)$ GeV, and $p_{T\mu\mu} > 200$ GeV
- Jets reconstructed from charged particles (excluding prompt leptons) with $p_T > 0.5$ GeV and $|\eta| < 2.5$ using the anti- k_t algorithm with $R = 0.4$

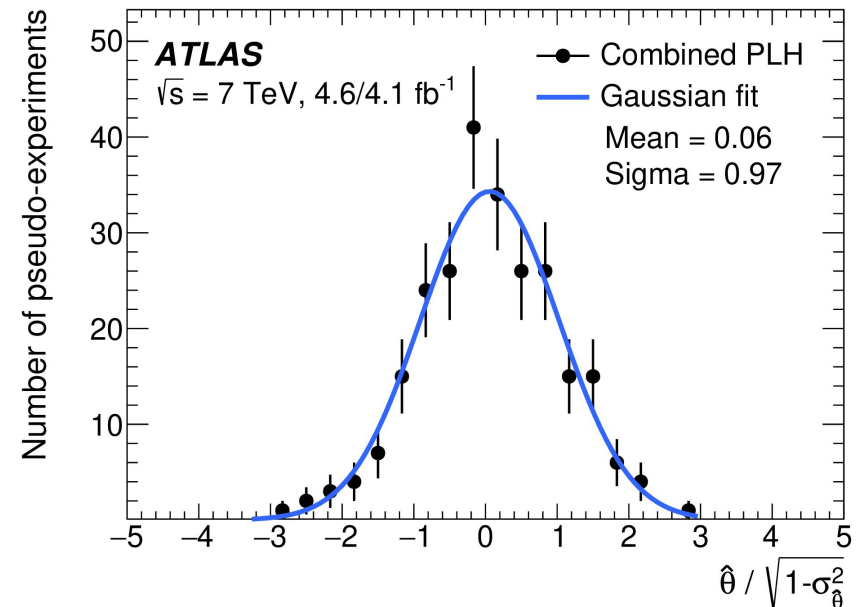
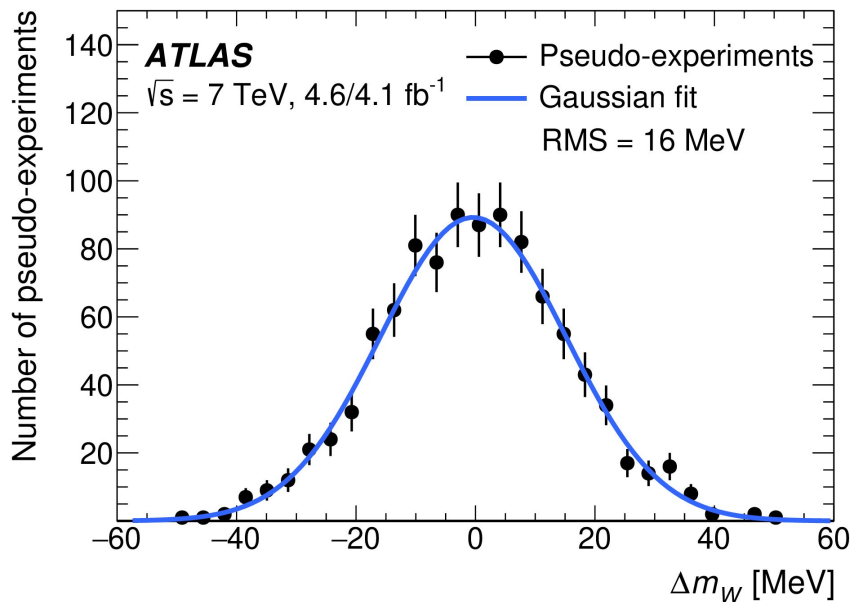
m_W : Comparison of statistical methods

- Compare fit results between χ^2 +offset method and PLH fit
- Using CT10nnlo PDF set (baseline in previous measurement)
- Total uncertainties reduced with PLH fit
- Combined lepton pfit: central T value shifted by 16 MeV



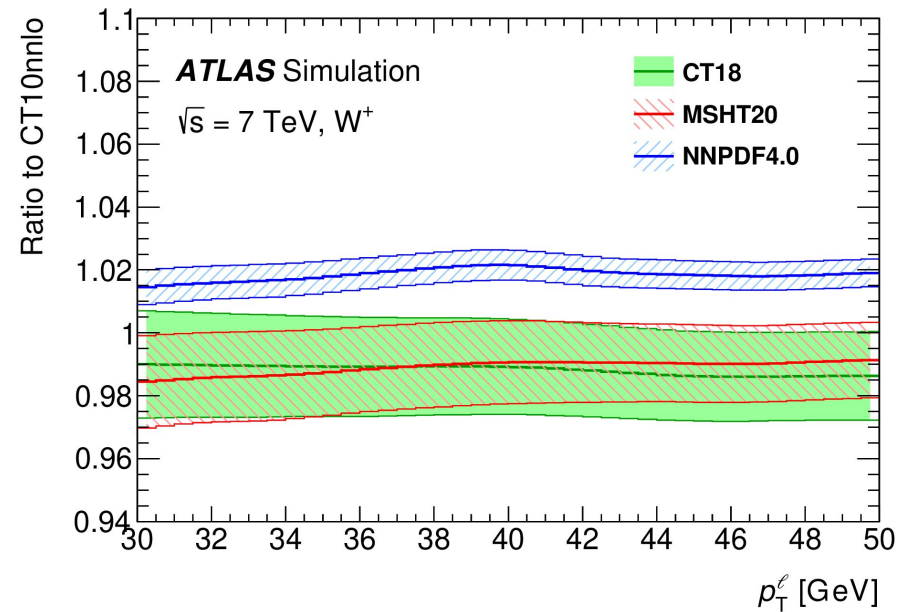
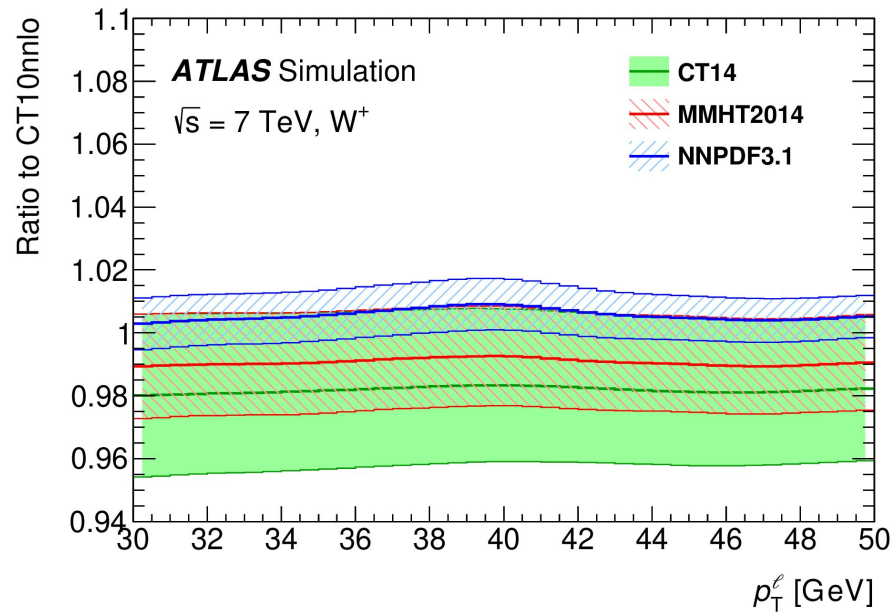
m_W : PLH fit checks

- Fit toys with random variations of nuisance parameters
- Central values for lepton p_T fit: 16 MeV spread \rightarrow χ^2 and PLH results agree at 1σ
- Distribution of nuisance parameter pulls consistent with normal distribution



PDF set updates

- Kinematic distributions extrapolated from CT10nnlo to more modern PDF sets using reweighting derived with POWHEG
- Impact on both shape and normalisation of distributions (esp. NNPDF sets!)



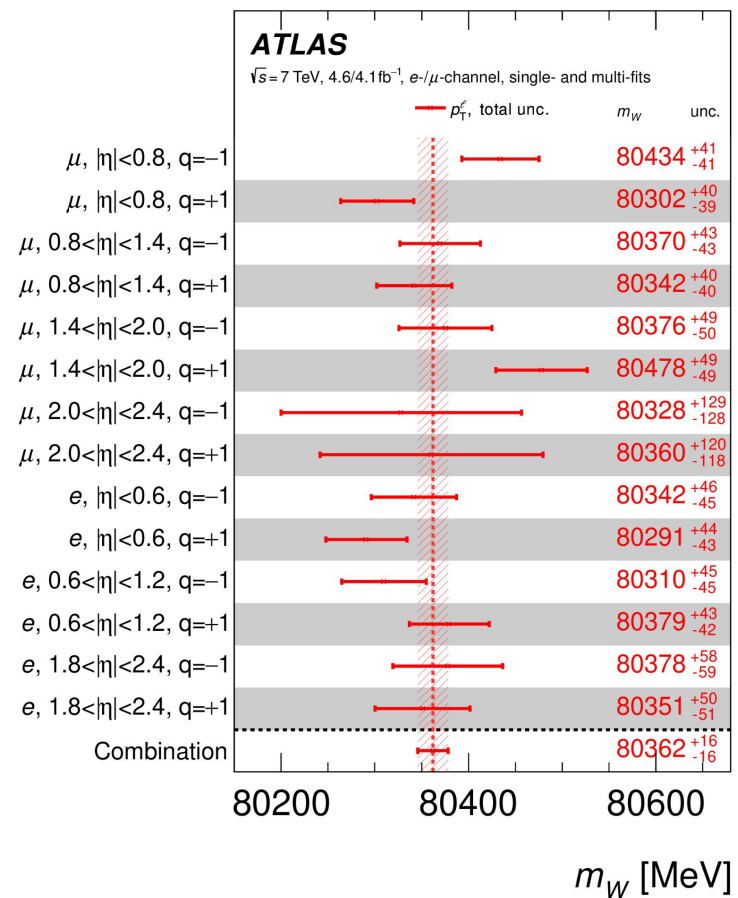
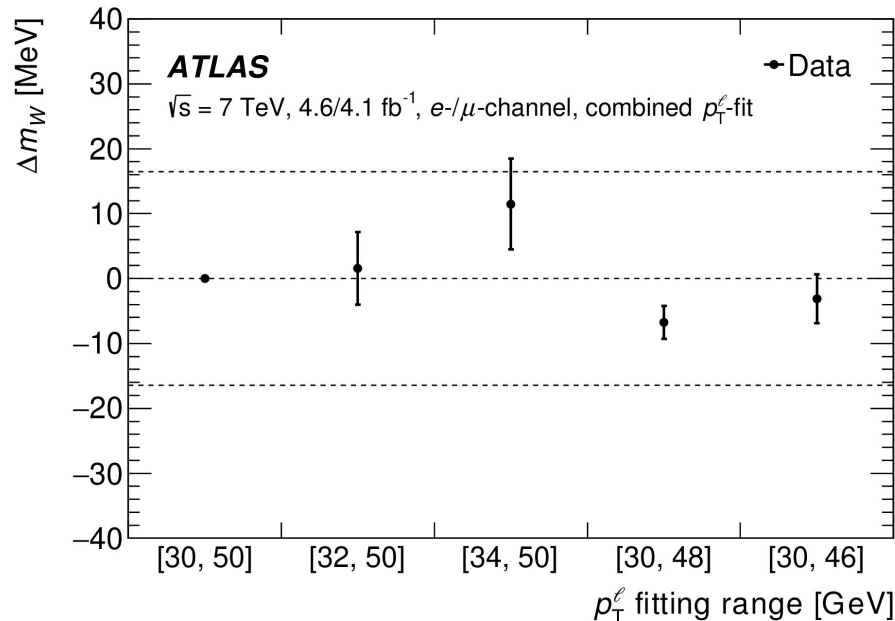
m_W : PDF dependence

- Results for most PDF sets agree within ~ 10 MeV (lepton p_T) or ~ 20 MeV (m_T)
- NNPDF sets yield significantly lower values than other sets
- Some dependence of total uncertainties on PDF set

PDF set	p_T^ℓ fit				m_T fit			
	m_W	σ_{tot}	σ_{PDF}	$\chi^2/\text{n.d.f.}$	m_W	σ_{tot}	σ_{PDF}	$\chi^2/\text{n.d.f.}$
CT14	80358.3	+16.1 -16.2	4.6	543.3/558	80401.3	+24.3 -24.5	11.6	557.4/558
CT18	80362.0	+16.2 -16.2	4.9	529.7/558	80394.9	+24.3 -24.5	11.7	549.2/558
CT18A	80353.2	+15.9 -15.8	4.8	525.3/558	80384.8	+23.5 -23.8	10.9	548.4/558
MMHT2014	80361.6	+16.0 -16.0	4.5	539.8/558	80399.1	+23.2 -23.5	10.0	561.5/558
MSHT20	80359.0	+13.8 -15.4	4.3	550.2/558	80391.4	+23.6 -24.1	10.0	557.3/558
ATLASpdf21	80362.1	+16.9 -16.9	4.2	526.9/558	80405.5	+28.2 -27.7	13.2	544.9/558
NNPDF3.1	80347.5	+15.2 -15.7	4.8	523.1/558	80368.9	+22.7 -22.9	9.7	556.6/558
NNPDF4.0	80343.7	+15.0 -15.0	4.2	539.2/558	80363.1	+21.4 -22.1	7.7	558.8/558

m_W : Fit results with CT18 PDF set

- Cross-checks done with separate combinations of e/ μ or W+/W- channels
- All consistent within 1σ
- No significant dependence on fitting ranges



Lepton p_T - m_T combination

- Fits using lepton p_T and m_T not statistically independent → combine with BLUE
- Correlation determined using toy variations of data and NPs
- Lepton p_T fits dominate combined results for m_W , m_T fit dominates for λ_W

PDF set	Correlation	weight (p_T^ℓ)	weight (m_T)	Combined m_W [MeV]
CT14	52.2%	88%	12%	80363.6 ± 15.9
CT18	50.4%	86%	14%	80366.5 ± 15.9
CT18A	53.4%	88%	12%	80357.2 ± 15.6
MMHT2014	56.0%	88%	12%	80366.2 ± 15.8
MSHT20	57.6%	97%	3%	80359.3 ± 14.6
ATLASpdf21	42.8%	87%	13%	80367.6 ± 16.6
NNPDF3.1	56.8%	89%	11%	80349.6 ± 15.3
NNPDF4.0	59.5%	90%	10%	80345.6 ± 14.9

PDF set	Correlation	weight (m_T)	weight (p_T^ℓ)	Combined Γ_W [MeV]
CT14	50.3%	88%	12%	2204 ± 47
CT18	51.5%	87%	13%	2202 ± 47
CT18A	50.0%	86%	14%	2184 ± 47
MMHT2014	50.8%	88%	13%	2182 ± 47
MSHT20	53.6%	89%	11%	2181 ± 47
ATLASpdf21	49.5%	84%	16%	2193 ± 46
NNPDF31	49.9%	86%	14%	2182 ± 46
NNPDF40	51.4%	85%	15%	2184 ± 46

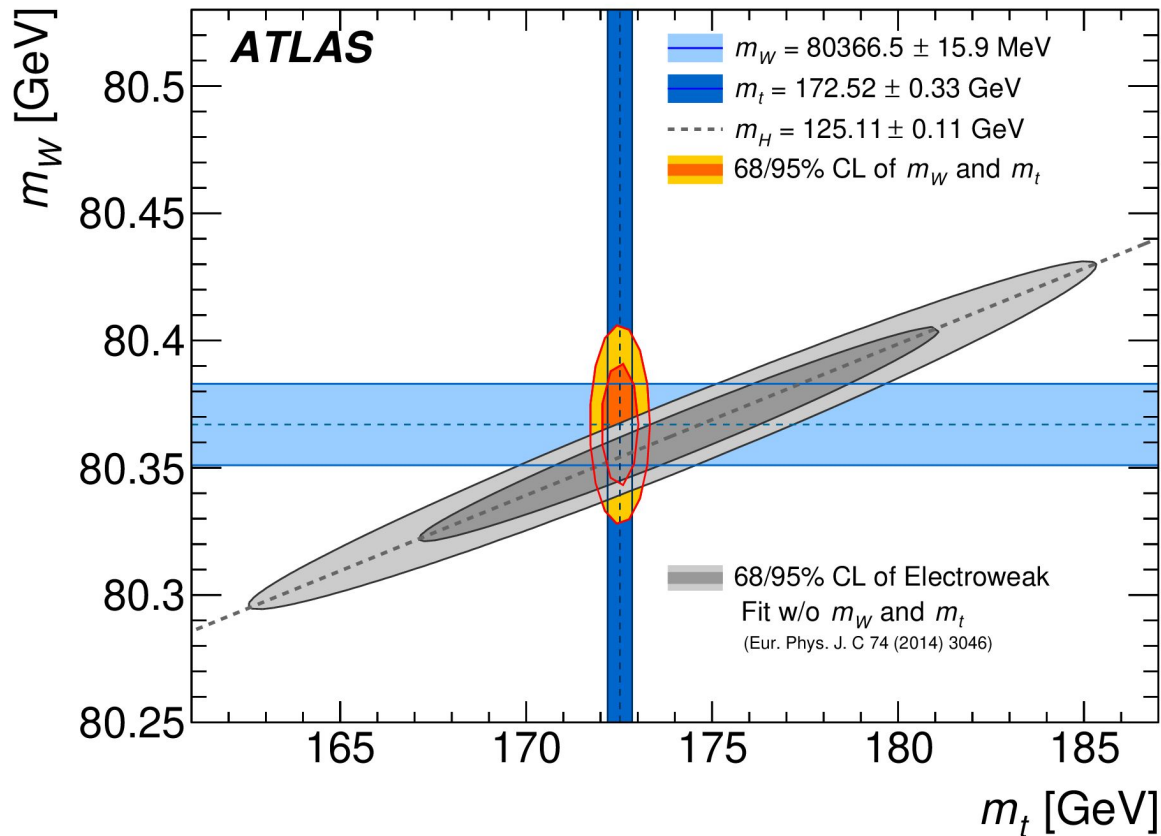
Uncertainty breakdown

m_W

Unc. [MeV]	Total	Stat.	Syst.	PDF	A_i	Backg.	EW	e	μ	u_T	Lumi	Γ_W	PS
p_T^ℓ	16.2	11.1	11.8	4.9	3.5	1.7	5.6	5.9	5.4	0.9	1.1	0.1	1.5
m_T	24.4	11.4	21.6	11.7	4.7	4.1	4.9	6.7	6.0	11.4	2.5	0.2	7.0
Combined	15.9	9.8	12.5	5.7	3.7	2.0	5.4	6.0	5.4	2.3	1.3	0.1	2.3

Γ_W

Unc. [MeV]	Total	Stat.	Syst.	PDF	A_i	Backg.	EW	e	μ	u_T	Lumi	m_W	PS
p_T^ℓ	72	27	66	21	14	10	5	13	12	12	10	6	55
m_T	48	36	32	5	7	10	3	13	9	18	9	6	12
Combined	47	32	34	7	8	9	3	13	9	17	9	6	18



The CL contours of the m_W and m_t indirect determinations from the global electroweak fit, compared to CL contours of the present ATLAS measurement of m_W , the ATLAS measurement of m_H and the LHC measurement of m_t

Monte Carlo Samples

In MC campaigns mc16a, mc16d, and mc16e:

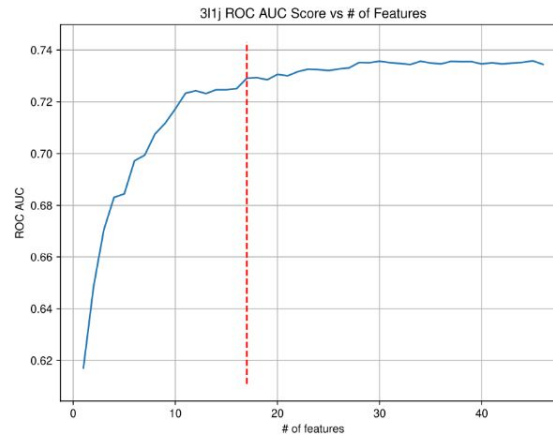
- Dedicated **VVV Signal samples** for both On-Shell (SHERPA 2.2.2) and Off-Shell (POWHEG+PYTHIA8+EVTGEN) included
 - $WWW \rightarrow 3\ell$ sample treated as background, $VH \rightarrow$ inclusive used as background with truth level filter to exclude signal processes
- **Largest backgrounds** VZ from qq (SHERPA 2.2.12) has NLO QCD accuracy in the matrix element for 0 and 1-jet states, LO accuracy for 2 and 3-jets states
 - $ggZZ$ (SHERPA 2.2.2) LO accuracy for 0 and 1-jet states
- $t\bar{t}V$ modelled in MADGRAPH5_AMC@NLO2.3.3+Pythia8.210
- $Z +$ jets (SHERPA 2.2.11) has 0, 1, 2 jets at NLO accuracy, & 3, 4, 5 jets at LO accuracy
- EFT Samples generated with MADGRAPH5_AMC@NLO2.7.3 at LO utilising reweighting tool

Detector-level correction weights applied to reconstructed events, including:

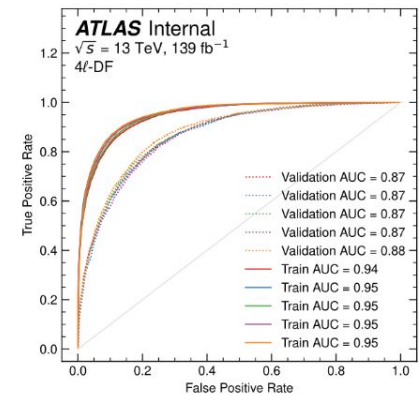
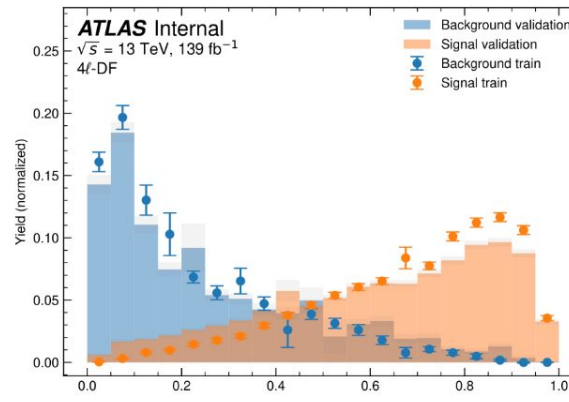
- Pile-up reweighting
- Muon SFs for reconstruction, identification and isolation
- Electron SFs for reconstruction, identification and isolation
- JVT
- FTag SFs and uncertainties, and inefficiency for jets not passing b-tagging

- All signal regions utilise MVA techniques to enhance sensitivity to VVZ processes
- All use XGBoost Boosted Decision Trees, each trained and optimised to each individual signal region across all final states (3ℓ +jets, 4ℓ & $\geq 5\ell$)
- Recursive Feature elimination used to minimise number of training features without compromising performance
- Input features used are visually inspected against data to ensure they are not badly modelled

MVAs



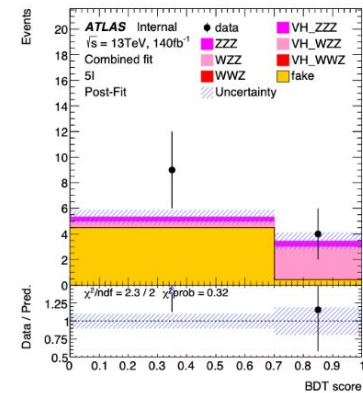
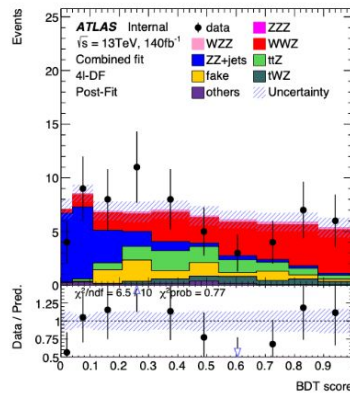
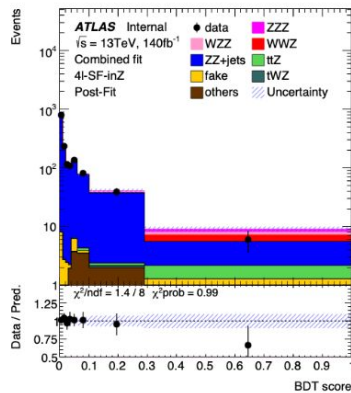
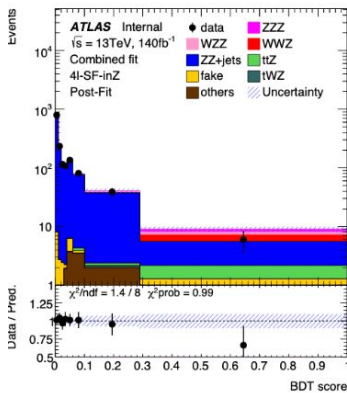
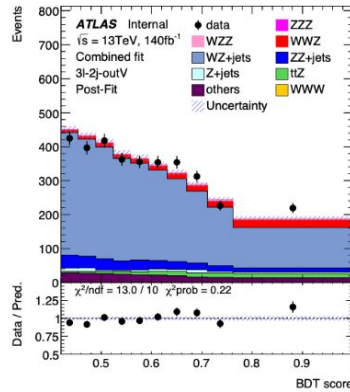
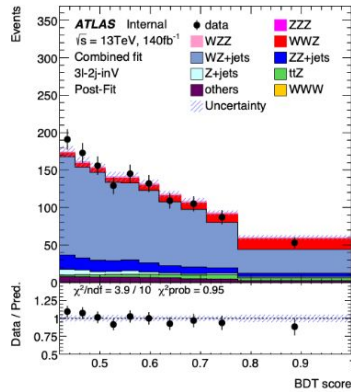
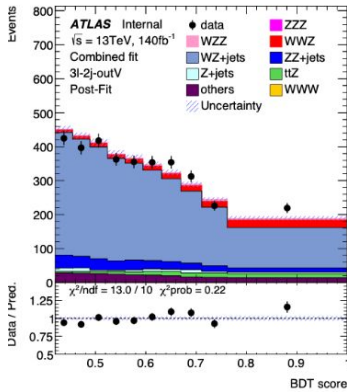
Variable name
$p_T^{Z\ell_1}, p_T^{Z\ell_2}, p_T^{\text{other } \ell_1}, p_T^{\text{other } \ell_2}$
$\eta_{Z\ell_1}, \eta_{Z\ell_2}, \eta_{\text{other } \ell_1}, \eta_{\text{other } \ell_2}$
$\Delta\phi_{Z\ell_1, Z}, \Delta\phi_{Z\ell_2, Z}, \Delta\phi_{\text{other } \ell_1, Z}, \Delta\phi_{\text{other } \ell_2, Z}$
$m_{\ell\ell}^{\text{best } Z}$
$m_{\ell\ell}^{\text{other}}$
$m_{4\ell}$
$p_T^{4\ell}$
$n(\text{jets})$
H_T^{lep}
H_T^{had}
H_T^{total}
E_T^{miss}
$\Delta\phi_{E_T^{\text{miss}}, Z}$
METSig



Unblinded Post-Fits

SR binning schemes optimised using TRexFitter
TransfoD algorithm with (5,5) or (1,1)

Channel	3l+jets	4l	5l
Signal Regions (TransfoD)	3l1j (5,5) 3l m _{jj} in V (5,5) 3l m _{jj} out V (5,5)	DF (5,5) SFInZ (5,5) SFOutZ (5,5)	VVZ (1,1)
Control Regions (# bins)	WZ (3) ttZ (1) Z+jets (1)	ZZ (3) ttZ (1)	
Normalisations	WZ (3) ttZ (1) Z+jets (1)	ZZ (3) ttZ (1)	



Sherpa Cross Sections

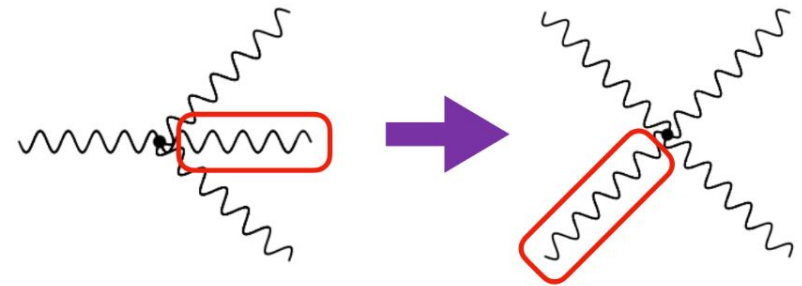
Process	Cross Section [fb]
<i>WWZ</i>	166
<i>WZZ</i>	56.4
<i>ZZZ</i>	14.1
<i>ZH → WWZ</i>	163
<i>WH → WZZ</i>	36.7
<i>ZH → ZZZ</i>	19.9

Extracted Cross Sections from Signal Strengths

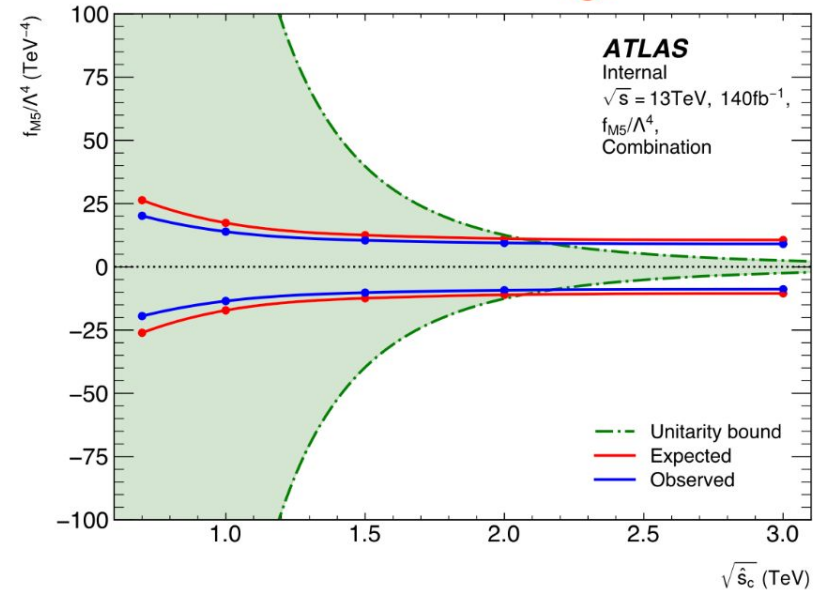
Process	Cross section (fb)	
	<i>VH</i> included in the signal	<i>VH</i> included in the background
<i>VVZ</i>	$655^{+94}_{-93} \quad ^{+98}_{-87}$	$377^{+57}_{-68} \quad ^{+70}_{-60}$
<i>WWZ</i>	$437^{+93}_{-92} \quad ^{+69}_{-56}$	$250^{+72}_{-60} \quad ^{+44}_{-46}$
<i>WZZ</i>	$198^{+110}_{-90} \quad ^{+71}_{-38}$	$121^{+68}_{-55} \quad ^{+45}_{-23}$

Clipping Scan

- Eboli Operator unitarity bounds are calculated for 2-to-2 scatterings, not natural for triboson
- Can use truth diboson invariant masses as proxy for $\sqrt{\hat{s}}$
- Clip EFT events where $Max(m_{VV}^{12}, m_{VV}^{23}, m_{VV}^{13}) > \sqrt{\hat{s}_c}$ on truth level at $E_c = 0.7, 1, 1.5, 2, 3$ TeV



Wilson Coefficient	Bound			
	1 operator		all 7 operators	
	For $\sqrt{s} < 1.5$ (3) TeV		For $\sqrt{s} < 1.5$ (3) TeV	
$\left \frac{f_{M,0}}{\Lambda^4} \right $	$\frac{32}{\sqrt{6}} \pi s^{-2}$	8.1 (0.5) TeV^{-4}	$\frac{2}{3}(72 + 5\sqrt{6}) \pi s^{-2}$	35 (2.1) TeV^{-4}
$\left \frac{f_{M,1}}{\Lambda^4} \right $	$\frac{128}{\sqrt{6}} \pi s^{-2}$	32 (2) TeV^{-4}	$8 \left(24 + \frac{\sqrt{6}}{5} \right) \pi s^{-2}$	122 (7.6) TeV^{-4}
$\left \frac{f_{M,2}}{\Lambda^4} \right $	$\frac{16}{\sqrt{2}} \pi s^{-2}$	7 (0.44) TeV^{-4}	$(24 + 5\sqrt{2}) \pi s^{-2}$	20 (1.3) TeV^{-4}
$\left \frac{f_{M,3}}{\Lambda^4} \right $	$\frac{64}{\sqrt{2}} \pi s^{-2}$	28 (1.7) TeV^{-4}	$96 \pi s^{-2}$	60 (3.7) TeV^{-4}
$\left \frac{f_{M,4}}{\Lambda^4} \right $	$32 \pi s^{-2}$	20 (1.2) TeV^{-4}	$4(5 + 8\sqrt{3}) \pi s^{-2}$	58 (3.6) TeV^{-4}
$\left \frac{f_{M,5}}{\Lambda^4} \right $	$64 \pi s^{-2}$	40 (2.5) TeV^{-4}	$64 \sqrt{3} \pi s^{-2}$	69 (4.3) TeV^{-4}
$\left \frac{f_{M,7}}{\Lambda^4} \right $	$\frac{256}{\sqrt{6}} \pi s^{-2}$	65 (4.0) TeV^{-4}	$\frac{64}{5}(24 + \sqrt{6}) \pi s^{-2}$	210 (13) TeV^{-4}



Unitarised Limits

Coefficient	Expected limit [TeV ⁻⁴]	Exp. E_C [TeV]	Observed limit [TeV ⁻⁴]	Obs. E_C [TeV]
f_{M2}/Λ^4	[-18, 17]	1.2	[-19, 19]	1.2
f_{M3}/Λ^4	[-28, 29]	1.5	[-28, 29]	1.5
f_{M5}/Λ^4	[-14, 14]	1.6	[-12, 12]	1.7
f_{M5}/Λ^4	[-11, 11]	2.1	[-9.1, 9.3]	2.2

